HOSTED BY

ELSEVIER

Available online at www.sciencedirect.com

ScienceDirect

journal homepage: http://www.journals.elsevier.com/journal-of-palaeogeography/

JOURNAL OF PALAEOGEOGRAPHY

Lithofacies palaeogeography and sedimentology

A review on palaeogeographic implications and temporal variation in glaucony composition

Santanu Banerjee, Udita Bansal, Anup Vilas Thorat*

Department of Earth Sciences, Indian Institute of Technology Bombay, Powai, Mumbai 400076, India

ARTICLE INFO

Article history:
Received 6 October 2015
Accepted 23 November 2015
Available online 12 December 2015

Keywords:
Glaucony
Glauconite
Evolutionary trend
Substrate
Palaeogeography
Faecal pellet

ABSTRACT

This study presents a review on palaeogeographic implications and temporal variations of glaucony covering both modern and ancient records. Phanerozoic glaucony preferably forms in a shelf depositional setting. Deep marine conditions and low seawater temperature discourage formation of glaucony. Around 75% of glaucony is recorded from the Cretaceous to the Holocene sediments, which are related to the abundance of the most common substrates, faecal pellets and bioclasts. TFe_2O_3 (total), Al_2O_3, K_2O and MgO contents of glaucony vary appreciably through geological time. While TFe_2O_3 content of most Mesozoic and Cenozoic glaucony exceeds 20%, it is always less than 20% in Precambrian varieties. High K_2O, Al_2O_3, MgO and low TFe_2O_3 distinguish the Precambrian glaucony from its Phanerozoic counterpart. Precambrian glaucony, preferably formed within a K-feldspar substrate, is always rich in potassium irrespective of its degree of evolution, while high K-content in Phanerozoic evolved glaucony indicates significant stratigraphic condensation. K_2O *vs.* TFe_2O_3 relationship of glaucony exhibits three different evolutionary trends corresponding to three common modes of origin. Depositional conditions may influence the composition of glaucony as slightly reducing conditions favour Fe enrichment, whereas oxidising conditions cause Fe depletion in glaucony.

1. Introduction

Glaucony is generally considered as a product of marine authigenesis, which is commonly associated with transgressive deposits and condensed sections (Odin and Matter, 1981; Amorosi, 1995, 1997; Amorosi and Centineo, 1997; Kitamura, 1998; Harris and Whiting, 2000; Giresse and Wiewióra, 2001; Hesselbo and Huggett, 2001; Meunier and El Albani, 2007; Banerjee *et al*., 2008, 2012a, 2012b; Chattoraj *et al*., 2009). Glaucony occurs typically in forms of 60 μm–1000 μm green clay aggregates in sedimentary rocks ranging in age from the Late Paleoproterozoic to the Holocene (Table 1; Webb *et al*., 1963; Odin and Matter, 1981; Dasgupta *et al*., 1990; Amorosi, 1994, 2012; Deb and Fukuoka, 1998; Lee *et al*., 2002; El Albani *et al*., 2005; Amorosi *et al*., 2007; Bandopadhyay, 2007; Banerjee *et al*., 2008, 2012a, 2012b, 2015; Chattoraj *et al*., 2009). Glaucony forms in a wide variety of substrates including faecal pellets, bioclasts, feldspar, mica and quartz. Although the stratigraphic implications of glaucony are fairly well understood because of its common association in sedimentary sequences representing simple

* *Corresponding author*.
E-mail address: santanu@iitb.ac.in (S. Banerjee).
Peer review under responsibility of China University of Petroleum (Beijing).
http://dx.doi.org/10.1016/j.jop.2015.12.001

Table 1 – Glaucony occurrences through different ages along with the background lithology, substrate and environmental interpretations.

Strata No.	Author	Age/Stratigraphic unit, location	Background lithology	Substrate	Environment/ Bathymetry
1	Wang (1983)	Holocene/Fuxiangraben Lake, Yunnan	Muds	–	Marine (35 m–150 m)
2	Seed (1965)	Holocene/South Island of New Zealand	Sands	Faecal pellets and alteration of micas	–
3	Vaz (2000)	Holocene/Offshore Cauvery Basin, India	Muds	–	Shelf to slope
4	Giresse *et al.* (2004)	Holocene/Gulf of Lion	–	–	–
5	Rothe (1973)	Holocene/Coast of Morocco, Canary and Cape Verde Islands	Marls	Foraminifera	–
6	Bell and Goodell (1967); Dill (1969)	Holocene/Atlantic continental shelf and slope of USA	Sands and muds	Faecal pellets, foraminifera and other bioclasts	Shelf to slope
7	Furquim *et al.* (2010)	Holocene/Lake of Nhecolândia (Pantanal wetland), Brazil	–	Micas	Lacustrine
8	Wang *et al.* (1985)	Holocene/Sanya Bay, South China Sea	–	Foraminifera and faecal pellets	–
9	Parker (1975); Birch (1979)	Holocene/Continental shelf off South Africa	Sands and muds	Foraminifera and faecal pellets	Shallow marine
10	Chen and Chen (1997)	Holocene/Taiwan Strait, South China Sea	–	–	Shallow marine
11	Giresse *et al.* (1988)	Holocene/Near the Congo river mouth	Sands and muds	Micas and clays	Inner shelf
12	Lee *et al.* (2002)	Holocene/Continental shelf off Yellow Sea	Sands and sandy muds	Faecal pellets	Intertidal to subtidal (10 m–80 m)
13	Basa *et al.* (1997)	Holocene/Sands of Dungeness	Sands and silts	–	Intertidal to subtidal
14	Martins *et al.* (2012)	Holocene/Continental shelf and upper slope of Portugal	Sands	Foraminifera and faecal pellets	Shelf (50 m–150 m)
15	Nelson and Bornhold (1984)	Holocene/Offshore Vancouver Island	Limestones and muds	Foraminifera and other bioclasts	Shelf (<200 m)
16	Mackenzie *et al.* (1988)	Holocene/Chatham Rise and Oamaru	–	–	Shelf
17	Hesse *et al.* (1971)	Holocene/Apulian shelf, Mediterranean	Limestone sands	Foraminifera and faecal pellets	Shelf
18	Ehlmann *et al.* (1963)	Holocene/Southeast coast of USA	Sands	Foraminifera and faecal pellets	Shelf (34 m–826 m)
19	Rongchuan *et al.* (1986); Lim *et al.* (2000)	Holocene/Offshore Yellow Sea, East Sea	Muds and sands	Foraminifera and faecal pellets	Middle shelf (~100 m)
20	Porrenga (1967)	Holocene/Niger delta, the Orinoco shelf and the shelf off Sarawak	Sands	Foraminifera, other bioclasts and faecal pellets	Outer shelf (125 m–250 m)
21	Dias and Nittrouer (1984)	Holocene/Offshore Portugal	Sands and biogenic limestones	Foraminifera	Outer shelf to shelf break (100 m–200 m)
22	Mendes *et al.* (2004)	Holocene/Guadiana shelf	Sandy and silty clays	Foraminifera and molluscs	Outer shelf (100 m–200 m)
23	Demirpolat (1991)	Holocene/Continental shelf off the Russian River	Sands	–	Outer shelf
24	Bornhold and Giresse (1985)	Holocene/Continental shelf off Vancouver Island	Muddy sands to sandy muds	Foraminifera and faecal pellets, mica	Outer shelf to upper slope (100 m–500 m)
25	Wigley and Compton (2007)	Holocene/Oligocene–Miocene/ Cape Canyon of South Africa	Sands or muds	Foraminifera and faecal pellets	Middle shelf to shelf edge (50 m–400 m)
26	Chen *et al.* (1980); Chen and Duan (1987)	Holocene/Continental shelf of East and South China Sea	–	Foraminifera	Outer shelf to upper slope (200 m–400 m)
27	Giresse and Wiewióra (2001); Baldermann *et al.* (2013)	Holocene/Deep sea, Ivory coast Ghana	–	Foraminifera	2100 m
28	Buatier *et al.* (1989)	Holocene/Galapagos spreading centre	Pelagic sediments	–	2500 m
29	Riedinger *et al.* (2005)	Holocene/Western continental margin off Argentina and Uruguay	Mudstones	–	Deep marine

Table 1 – (continued)

Strata No.	Author	Age/Stratigraphic unit, location	Background lithology	Substrate	Environment/ Bathymetry
30	Thompson and Hower (1975)	Holocene/Offshore California	Sands	Faecal pellets	–
31	Odin and Matter (1981)	Pleistocene–Holocene/Senegal and Gulf of Guinea	Sands	Bioclasts, faecal pellets, alteration of micas, quartz, chert and feldspars	–
32	Parry and Reeves (1966)	Pleistocene–Holocene/Pluvial Lake Mound, USA	Sands and dolomites	Faecal pellets	Lacustrine
33	Bandy (1972)	Pleistocene/Lomita Marl, California	Marls	–	–
34	Compton and Wiltshire (2009)	Pleistocene/Western shelf of South Africa	–	–	–
35	Bau *et al.* (2004)	Pleistocene/Cape Cod aquifer, Massachusetts, USA	–	–	–
36	Altaner *et al.* (2013)	Pleistocene (~55 Ka)/Mount Epomeo Green Tuff, Italy	Tuffs	–	–
37	Giresse *et al.* (2015)	Late Pliocene–Early Quaternary/ Cedrino paleovalley (Orosei area)	–	–	–
38	Ly (1981)	Pleistocene/Central and eastern coasts of Ghana, West Africa	Sands	–	Upper shoreface (<25 m)
39	Merriman (1983); Humphreys and Balson (1985)	Pliocene–Early Pleistocene/Red Crag and Coralline Crag Formation (East Anglia, North Sea)	Shelly sands	Bioclasts	Shallow marine
40	Kitamura (1998)	Early Pleistocene/Omma Formation, offshore Japan		–	50 m–120 m
41	Arning *et al.* (2009)	Pleistocene–Holocene/Offshore Peru	Sandstones and limestones	–	Shelf
42	Saito *et al.* (1989)	Pleistocene–Holocene/Shelf and upper slope off Sendai, Northeast Japan	Sands and sandy muds	–	Shelf
43	Rao *et al.* (1993, 1995)	Late Pleistocene–Holocene/ Eastern and southwestern continental margin of India	Sandy clays, clayey sands	Foraminifera and faecal pellets	Shelf and slope (20 m –280 m)
44	Barusseau *et al.* (1988)	Pleistocene–Holocene/Shelf areas off Congo, Senegal	Sandstones	Faecal pellets and ostracoda	Middle shelf
45	Brandano and Civitelli (2007)	Plio-Pleistocene/Pontinian Islands, Tyrrhenian Sea	Sands and silts	Foraminifera, gastropod, bryozoa, sponge spicule and echinoderm	Middle shelf
46	Carter (1975)	Late Pleistocene–Holocene/ Hawkes Bay–Wairarapa Shelf, New Zealand	–	Faecal pellets foraminifera	Middle shelf to outer slope (130 m–300 m)
47	McMaster and LaChance (1968)	Pleistocene/Northwestern African Shelf	Sands	–	Shelf and upper slope
48	Cook and Marshall (1981)	Late Pleistocene/East Australian Continental Shelf	Muds	Faecal pellets and bioclasts	Outer shelf (200 m–300 m)
49	Burnett (1980)	Holocene/Peru and Chile offshore	Diatomaceous sediments	Faecal pellets	Deep marine (300 m–400 m)
50	Howe *et al.* (1997)	Pliocene–Mid-Pleistocene/South Atlantic Ocean	Sandstones	Faecal pellets	Deep marine (1000 m –3000 m)
51	Odin and Matter (1981)	Mio-Pliocene/Shelf of Northwest Spain	Sands	Bioclasts, faecal pellets, alteration of micas, quartz, chert and feldspars	–
52	Harris and Whiting (2000)	Mio-Pliocene/US Mid-Atlantic Margin	–	–	–
53	Huisman *et al.* (1997); Griffioen *et al.* (2012)	Miocene/Breda Formation, Netherland	Sands	–	Shallow marine and coastal
54	John *et al.* (2011)	Miocene/Cores from Northeast Australian offshore	Limestones and marls	–	Middle, outer shelf to upper slope (100 m–350 m)
55	Vandenberghe *et al.* (2014)	Miocene/Diest Formation	Sandstones	–	–
56	Gier *et al.* (2008)	Early–Middle Miocene/Vienna Basin	Sandstones	–	Shallow marine

(*continued on next page*)

Table 1 – (continued)

Strata No.	Author	Age/Stratigraphic unit, location	Background lithology	Substrate	Environment/ Bathymetry
57	Van Delft *et al.* (1990)	Middle Miocene/Miste Bed, Rupel Formation	Clays and sands	–	–
58	Chen (1983)	Miocene/Xiayang Formation	Arkosic sandstones	–	Shelf
59	De Ros *et al.* (1997)	Miocene/Northwest African margin offshore	Sandy mudstones and sandstones	Foraminifera and faecal pellets, mica	Middle shelf to upper slope
60	Fischer (1987); Stille and Fischer (1990)	Miocene/Upper Marine Molasse	Sands, clays and marls	Altered biotite	Marine (200 m–600 m)
61	Asensio *et al.* (2012)	Miocene/Lower Guadalquivir Basin	Siltstones and sandstones	–	Inner shelf to middle slope (50 m–600 m)
62	Lantzsch *et al.* (2010)	Mio-Holocene/Offshore Iberia	Sandstones	–	Outer shelf
63	Özgüner and Varol (2009)	Miocene/Manavgat Basin, Anatolia	Pelagic limestones	Foraminifera and hardground borings	Outer shelf
64	Amorosi *et al.* (1997)	Early Miocene/Visone Formation	Sandstones	–	Outer shelf
65	Charpentier *et al.* (2011)	Miocene–Pleistocene/Offshore Nicoya Peninsula Costa Rica	–	–	Abyssal plain
66	Muza and Wise (1983)	Miocene/Falkland Plateau	Pelagic limestones	Foraminifera and faecal pellets	Abyssal plain
67	Föllmi and Breymann (1992)	Miocene–Pleistocene/Japan Sea	Diatom-rich limestones	Faecal pellets	Abyssal plain
68	Hower (1961)	Oligocene/Byram Formation	Marls	Faecal pellets	–
69	Banerjee *et al.* (2012a)	Oligocene/Maniyara Fort Formation	Shales	Foraminifera and faecal pellets	Lagoonal
70	Porrenga (1968)	Oligocene/Aardebrug, Belgium	Sandstones	Illite-montmorillonite clays	Lagoonal and hypersaline lake
71	Boukhalfa *et al.* (2015)	Oligocene/Fortuna Formation	–	–	Inner shelf and lagoonal
72	Dix and Parras (2014)	Oligocene–Early Miocene/San Julián Formation	Hardgrounds in limestones	–	Shallow marine
73	Rasmussen and Dybkjaer (2005)	Oligocene/Ringkøbing-Fyn High, Denmark	Mudstones	–	Inner to outer shelf
74	Skiba *et al.* (2014)	Oligocene/Góra Puławska, Poland	Quartzose sandstones	–	–
75	Lewis and Belliss (1984)	Oligocene–Miocene/Gee Greensand, Otekaike Limestone, Kokoamu Greensand	Sandstones and limestones	–	Shelf
76	Chang *et al.* (2008)	Oligocene–Miocene/Shuichangliu Formation, Changhukeng Formation, Tsukeng Formation, Takeng Formation	Siltstones and mudstones	Faecal pellets	–
77	Hesselbo and Huggett (2001)	Oligocene–Pliocene/Offshore New Jersey	Mudstones and sandstones	Faecal pellets	Shallow to deep marine (100 m–1000 m)
78	Kelly and Webb (1999); Kelly *et al.* (2001)	Oligocene–Miocene/Torquay Group	Bioclastic limestones and mudstones	Faecal pellets and bioclasts	Middle shelf
79	Tóth *et al.* (2010)	Late Oligocene/Eger Formation	Sandstones	Faecal pellets and foraminifera and echinoderma	Outer shelf to slope (100 m –1000 m)
80	Tazaki and Fyfe (1992)	Oligocene/Izu–Bonin sediments along Bonin–Mariana Trench	Volcanogenic sandstones	–	Deep sea
81	Jiang *et al.* (2007)	Eocene/Half-graben lake basin (Shulu Sag), North China	Mudstones, calcareous shales	–	Deep lake
82	Huggett and Cuadros (2010)	Eocene–Oligocene/Seagrove Member	Marls/siltstones/clay minerals	–	Lacustrine
83	Odin and Matter (1981)	Eocene–Oligocene/Paris Basin	Sandstones, shales, limestones	Bioclasts, faecal pellets, alteration of micas, quartz, chert and feldspars	–

Table 1 – (*continued*)

Strata No.	Author	Age/Stratigraphic unit, location	Background lithology	Substrate	Environment/ Bathymetry
84	Hower (1961); Thompson and Hower (1975)	Eocene/Bashi Formation, Pierson Formation, Gatchell Formation, Matalani Formation, Domengine Formation, Carrizo Formation, Reklaw Formation, Moody's Branch Formation, Winona Formation, Weches Formation	Sandstones, marls, cherts	Faecal pellets	–
85	Thompson and Hower (1975)	Eocene/Cayat Formation, Zilpha Formation, Nanafalia Formation, Landrum Formation	Sandstones, shales, marls	Faecal pellets	–
86	Ćosović and Drobne (1995)	Eocene/Istria	–	Faecal pellets and foraminifera	–
87	Czuryłowicz *et al.* (2014)	Eocene–Oligocene/Lubartów area, eastern Poland	Sandstones	–	–
88	Velde and Medhioub (1988)	Eocene/Peeler Ranch Well, Texas	Sandstones and mudstones	–	–
89	Amaral (1967)	Eocene–Oligocene/Marajó Basin and Sergipe–Atagoas Basin	Fine sandstones and siltstones	Faecal pellets	–
90	Das and Duarah (1993)	Eocene/Siju Formation	Impure limestones	Foraminifera	–
91	Baioumy (2007)	Eocene/Hamra Formation	Sandstones, shales	Faecal pellets	Shallow marine
92	Sarmah and Borgohain (2012)	Eocene/Narpuh Sandstone	–	–	–
93	Hower (1961); Strickler and Ferrell (1990)	Eocene/Wilcox Sandstone	Sandstones	–	Shallow marine/littoral
94	Fanning *et al.* (2010)	Eocene/Nanjemoy Formation	Sands	Faecal pellets	Shallow marine
95	Clark and Robertson (2005)	Eocene/Gűműs Member	Nummulitic limestones	Bioclasts	Shallow marine
96	Harding (2014)	Eocene/Main Glauconite Bed	Mudstones	–	Shallow marine
97	Rasser and Piller (2004)	Eocene/Austria	Algal limestones	Foraminifera	Shallow marine
98	Sarma and Basumallick (1979)	Eocene/Sylhet Limestone	Limestones	Foraminifera and faecal pellets	Shallow marine
99	Geptner *et al.* (2008)	Eocene–Oligocene/Amanin Formation	Volcanogenic sandstones, mudstones	Clays	Shallow marine
100	Tlig *et al.* (2010)	Eocene/El Garia Formation, Metlaoui Group, Tunisia	Impure limestones	–	Shallow marine
101	Newman *et al.* (2013)	Eocene/Lambeth Group	Sands	Faecal pellets	–
102	Aitchison (1988)	Eocene/Tapui Glauconitic Sandstone	Sandstones	Foraminifera and faecal pellets	Inner shelf
103	Vander Lingeb *et al.* (1978)	Eocene/Eyre Sand Group	Sandstones	Foraminifera and faecal pellets, sponge spicules	Inner shelf
104	Huggett *et al.* (2010)	Eocene/Claiborne Group	Clayey sandstones and shales	Foraminifera and faecal pellets	Inner to middle shelf
105	Banerjee *et al.* (2012b)	Eocene/Harudi Formation	Shales	Foraminifera and faecal pellets	Middle shelf (40 m–60 m)
106	Plint (1983)	Eocene/Bracklesham Formation	–	–	–
107	Marivaux *et al.* (2014)	Eocene/Fortuna Formation	Shales	–	Subtidal to upper intertidal
108	Chattoraj *et al.* (2009)	Eocene/Naredi Formation	Shales	Foraminifera and faecal pellets, feldspars	Middle shelf
109	Ćosović *et al.*, 2004	Middle Eocene/Adriatic limestone platform	Impure limestone	Foraminifera and faecal pellets	Middle to outer ramp
110	MacGregor (1983)	Eocene–Oligocene/Waitakere Formation and Tiropahi Limestone	Impure limestone	Foraminifera, bryozoa and bored bioclasts	Middle to outer shelf
111	Schweitzer *et al.* (2005)	Eocene/Gračišće Region	Packstones	–	Outer ramp
112	Hughes and Whitehead (1987)	Eocene/Barton Formation	Sandstones	Quartz and chert	Deep shelf to slope

(*continued on next page*)

Table 1 – (continued)

Strata No.	Author	Age/Stratigraphic unit, location	Background lithology	Substrate	Environment/ Bathymetry
113	Morton *et al.* (1984)	Early Eocene–Middle Miocene/ Offshore Ireland	Chalks	Foraminifera and radiolaria	Abyssal plane
114	Kalia and Kintso (2006)	Late Paleocene–Early Eocene/ Jaisalmer Basin	–	–	–
115	Hower (1961)	Paleocene/Mahele Formation, Martinez Formation, Lodo Formation, Mathews Formation	Sandstones and marls	Faecal pellets	–
116	Franzosi *et al.* (2014)	Paleocene/Salamanca Formation	Sands	Quartz and feldspars	–
117	Lurcock and Wilson (2013)	Paleocene/Abbotsford Formation	–	–	–
118	McRae and Lambert (1968); Fitch *et al.* (1978); Knox (1979); Merriman (1983)	Paleocene–Eocene/Thanet beds, Reculver sands, Oldhaven beds, Woolwich beds, East Kent	Sandstones	Faecal pellets and flints	–
119	Friis *et al.* (2007)	Paleogene/Stavanger Platform, Danish North Sea	–	–	–
120	Bajda and Kłapyta (2013)	Cenozoic/The Lubartowska Lowland	Sands	–	–
121	Chen (1980); Wu *et al.* (1997); Ge (2004)	Paleogene/Shahejie Formation, Huagong Formation, East China Sea	–	–	–
122	Mancini and Tew, (1993)	Early Paleocene/Naheola Formation, Porters Creek Formation	Sandstones and marlstones	–	Shallow marine, near coast
123	Purdy *et al.* (1987)	Paleocene/Aquia Formation	Sandstones	–	Shallow marine
124	Duarte and Martínez, (2002)	Paleocene/Sepultura Formation	Sandstones	Foraminifera and faecal pellets, mica	Shallow marine
125	Sorrentino *et al.* (2014)	Early Paleogene/Red Bluff Tuff Formation	Tuffs	–	Shallow marine
126	Samanta *et al.* (2013)	Paleocene–Eocene/Cambay shale	Shales	–	Inner shelf
127	Stassen *et al.* (2015)	Paleocene–Eocene/Vincentown Formation, Manasquan Formation	Sandstones	–	Outer neritic (100 m–110 m)
128	Dill *et al.* (1996)	Paleocene–Eocene/North German Basin	Siltstones and shales	–	Shelf (60 m–100 m)
129	Amouric and Parron (1985); Parron and Amouric (1990)	Paleocene/Eboinda Region, Ivory Coast	Black shales	–	Deep marine
130	Sprong *et al.* (2013)	Paleocene/Kasserine Island	Marls and shales	–	Deep marine
131	Díez-Canseco *et al.* (2014)	Cretaceous–Paleogene boundary/ Lower Tremp Formation	–	–	–
132	Ferrow *et al.* (2011)	Cretaceous–Paleocene/Conway Formation	–	–	–
133	Valanciene *et al.* (2014)	Late Cretaceous–Paleogene/ Sventoji glauconite deposit, Lithuania	–	–	–
134	Mc Conchie and Lewis (1980)	Late Cretaceous–Paleogene/South Island of New Zealand	–	Faecal pellets, micas, sponge spicules and radiolaria	–
135	Cas *et al.* (1989)	Late Cretaceous–Paleogene/ Waiareka–Deborah Formation	Volcaniclastic rocks, mudstones and sandstones	Alteration of basaltic glass	Outer shelf
136	Hower (1961)	Cretaceous/Vidono Formation, Temblador Formation, Panoche Formation, Eutaw Formation, Ripley Formation, Prairie Bluff Formation	Sandstones, marls, cherts	Faecal pellets	–
137	Thompson and Hower (1975)	Cretaceous/Bornholm Island, Taft Hill Formation	Sandstones	Faecal pellets	–
138	McRae and Lambert (1968)	Aptian–Albian/Lower Greensand Formation	Sandstones	Faecal pellets	–
139	Morton and Long (1980)	Late Cretaceous/Dessau Formation, Austin, Texas	–	–	–

Table 1 – (continued)

Strata No.	Author	Age/Stratigraphic unit, location	Background lithology	Substrate	Environment/ Bathymetry
140	Salamon (2007)	Cenomanian/Strata in the Wolbrom–Miechów area, South Poland	Sandstones	–	–
141	Selby (2009)	Cenomanian/Section at Pays de Caux, Normandy, France	–	–	–
142	Cimbálníková (1971)	Late Cretaceous/Bohemia	–	–	–
143	Amorosi *et al.* (2012)	Cenomanian–Santonian/Sierra de Guadarrama Formation	Mudstones	–	–
144	Courbe *et al.* (1981)	Turonian/Maine-et-Loire, France	Sandstones	–	–
145	Cao *et al.* (2010)	Cretaceous/Unclassified, eastern Heilongjiang Province	Sandstones	–	–
146	Chen (1980)	Cretaceous/Yaojiazu Formation	Sandstones	–	–
147	Baker *et al.* (1997)	Cretaceous/Bonaparte and northern Carnarvon Basins, offshore Australia	–	–	–
148	Robert (1973)	Cenomanian/Cormes and Villers Formation, France	Sandstones	–	–
149	Prélat *et al.* (2015)	Cenomanian–Campanian/Svarte, Tryggvason, Lower Kyrre Formation	Sandstones	–	–
150	García-García *et al.* (2011)	Barremian–Aptian/Cerrajón Formation	–	–	–
151	Fiet *et al.* (2006)	Hauterivian–Albian/Vocontian basin (Southeast, France)	–	–	–
152	Li *et al.* (2012)	Albian/Gajie Formation	Sandstones	Quartz	Shelf
153	Lu and Smith (1996); Smith *et al.* (1996)	Early Cretaceous/Jonava region, Central Lithuania	–	–	–
154	Ireland *et al.* (1983)	Albian/Glauconitic Sandstone or Blusky Formation, Canada	Sandstones	Faecal pellets	–
155	Jamoussi (1991); Srasra and Trabelsi-Ayedi (2000)	Barremian/Unclassified, Gafsa area, Tunisia	Sands	–	–
156	Lorenzen *et al.* (2013)	Aptian/Stratotype at Roquefort-La Bédoule, Southeast France	Limestones, marls, marly limestones	–	–
157	Wortmann *et al.* (2004)	Aptian/Rehbreingraben Formation	Turbidite sandstones	–	–
158	Vijan *et al.* (2000)	Albian/Goru and Pariwar Formation	–	–	–
159	Reeder *et al.* (1972)	Albian/Clearwater Formation	Sandstones	–	–
160	Debrabant and Paquet (1975)	Albian/Sierra de Espufia, southern Spain	–	–	–
161	Guo (1991)	Barremian/Kizilsu Group	Sandstones, greywackes	–	–
162	El Albani *et al.* (2004, 2005)	Early Cretaceous/Berrisian of Aquitaine Basin	Claystones, dolomitic mudstones	Faecal pellets, feldspar and clay minerals	Lagoon and estuary
163	El-Azabi and El-Araby (2007); Farouk (2015); Zalat *et al.* (2012)	Coniacian–Santonian/Matulla Formation, Egypt	Shales	Faecal pellets	Lagoon/shoreface
164	Glenn and Arthur, 1990; Baioumy (2007); Rifai and Shaaban (2007); Ahmad *et al.* (2014)	Campanian–Maastrichtian/Duwi Formation, Egypt	Sandstones	Faecal pellets, alteration of micas and clay minerals	Shallow marine
165	Caracciolo *et al.* (2011)	Turonian–Coniacian/Peruc –Korycany Formation	Sandstones	–	Shoreface
166	Saha *et al.* (2010)	Late Cretaceous/Lameta Formation	Sandstones	–	Subtidal, estuarine (<200 m)
167	Walker and Bergman (1993); Amorosi (2011)	Campanian/Shannon Sandstone	Sandstones	Quartz	Shoreface, shallow marine
168	Meshri and Comer (1990)	Albian/Glauconite Sandstone, Canada	Sandstones	Faecal pellets	Deltaic

(continued on next page)

Table 1 – (continued)

Strata No.	Author	Age/Stratigraphic unit, location	Background lithology	Substrate	Environment/ Bathymetry
169	Wood and Hopkins (1992)	Early Cretaceous/Glauconitic Member in Badger fields, Canada	–	–	–
170	Bitschene *et al.* (1992)	Late Cretaceous/South Kerguelen Plateu ODP leg 120 (Site 748)	Sandstones, siltstones, claystones, limestones	Foraminifera and faecal pellets, mica	Nearshore, inner to outer shelf
171	Parize *et al.* (2005)	Early Cretaceous/Saint Laurent de l'Escarène, Southeast France	Sandstones and siltstones	–	Shoreface
172	Varol *et al.* (2000)	Aptian–Cenomanian/Kilimli, Sapca and Cemaller Formations	Sandstones and shales	Faecal pellets, quartz and feldspar	Shoreface to middle shelf
173	Mishra and Sen (2001); Tewari *et al.* (2010)	Maestrichtian/Mahadek Formation, India	Sandstones	–	Shallow marine
174	Martinec *et al.* (2010)	Cenomanian/Zamel Sandstone, Bohemia	Sandstone	–	Shallow marine
175	Harris and Bottino (1974); Harris (1976); Legrand (1989)	Maastrichtian/Peedee Formation	Sandstones, claystones	Bioclasts and faecal pellets	Open marine shelf deposition
176	Metwalli and Abdel-Hadi (1975)	Turonian/Abu Qada Formation	Calcareous sandstones	–	Shallow marine
177	Anan (2014)	Cenomanian–Turonian/Raha Formation, Egypt	Sandstone	Faecal pellets	Shallow marine
178	Odin *et al.* (1977)	Aptian, Albian and Cenomanian/ Paris Basin	Sandstones	Faecal pellets	Shallow marine
179	Pasquini *et al.* (2004)	Valanginian–Cenomanian/Nice Arc, France	Marls, sandstones	–	Shallow marine
180	Henderson (1998)	Aptian–Turonian/Darwin, Marligar, Wangarlu, Moonkinu Formations	Sandstones	Quartz and micas	Shallow marine
181	Bansal and Banerjee (2014)	Maastrichtian/Lameta Bed	Sandstones	Faecal pellets, feldspars	Shallow marine
182	Amireh (1997); Amireh *et al.* (1998); Jarrar *et al.* (2000)	Albian–Cenomanian/Kurnub Group	Limestones, mudstones	–	Shallow marine
183	Loveland (1981); Garrison *et al.* (1987); Carson and Crowley (1993)	Albian–Cenomanian/Upper Greensand Formation and Beer Head Limestone	Sandstones, marls, limestonse, chalks	Foraminifera and faecal pellets, quartz	Shallow marine
184	Yilmaz *et al.* (2012)	Barremian/Sakarya Zone, Turkey	Limestones, shales	–	Shallow marine
185	Godet *et al.* (2010, 2011)	Hauterivian–Barremian/Urgonian platform, Switzerland	Limestones	–	Shallow marine
186	Orberger and Pagel (2000)	Albian/Drill core MAR 501 Nimes fault, Cevennes fault, Southeast France	Sandstones and siltstones	Faecal pellets	Shallow marine
187	Najarro *et al.* (2011)	Aptian/Patrocinio Formation	Impure limestones	–	Shallow marine
188	Maher *et al.* (2004)	Aptian–Albian/Carolinefjellet Formation	Sandstones	–	Shallow marine
189	Rathore *et al.* (1999)	Albian/Ukra member, Bhuj Formation, India	Sandstones and shales	–	Shallow marine
190	Humez *et al.* (2013)	Albian/Paris basin, France	Sandstones	Faecal pellets	–
191	Vasković *et al.* (2010)	Cretaceous/Belgrade and Carpatihan areas, East Serbian	Sandstones	–	Shallow marine
192	Ashuri *et al.* (2010); Sharafi *et al.* (2013)	Albian–Cenomanian/Aitamir Formation	Shales	Quartz, chert and feldspar	Shoreface and outer shelf
193	Banning *et al.* (2013)	Santonian/Haltern Formation	Sandstones	Faecal pellets	Shallow marine (40 m–60 m)
194	Neill and Ruffell (2004)	Coniacian–Santonian/Hibernian Greensand Formation	Sandstones	–	–
195	Khalifa (1983); Baioumy and Boulis (2012a, 2012b)	Campanian/Qusseir Formation; Cenomanian/Bahariya Formation	Shales, sandstones	Alteration of micas or clays	Inner shelf
196	Michalík *et al.* (2012)	Albian/ the Manín Unit, central Western Carpathians, Slovakia	Limestones	Foraminifera	Shallow marine (50 m–60 m)

Table 1 – (*continued*)

Strata No.	Author	Age/Stratigraphic unit, location	Background lithology	Substrate	Environment/ Bathymetry
197	Gebhart (1982)	Albian/Near Clars, Escragnolles, Var, Southeast France	–	–	Marine, condensed zone
198	Hower (1961); Boyer *et al.* (1977); Montag and Seidemann (1981); Olsson (1989); Barringer *et al.* (2010); Obasi *et al.* (2011)	Cretaceous/Bass River Formation, Merchantville Formation, Marshalltown Formation, Navesink Formation, New Egypt Formation, Tinton Formation, Hornerstown Formation	Shales, sandtones	Faecal pellets	Shoreface and shelf environment
199	Rousset *et al.* (2004)	Albian–Cenomanian/Dent de Marcoule, Southeast France	Siltstones and sandstones	–	Shelf/Transgressive
200	Dypvik *et al.* (1992)	Berriasian/Myklegardfjellet Bed, Spitsbergen, Norway	Silty clays and siltstones	–	Marine shelf/Transgression
201	Garzanti *et al.* (1989)	Albian/Giumal Greensand Formation	Sandstones	Faecal pellets and volcanic fragments	Shelf
202	Delamette (1989)	Albian/Aravis Formation	Sandstones	Clays	Shelf (50 m–150 m)
203	Breheret (1991)	Mid-Cretaceous/Vocontian Basin, Southeast France	Black shales	Faecal pellets	–
204	Farouk (2015)	Cenomanian/Galala Formation, Galala Plaetauex, Egypt	Sandstones, shales	Faecal pellets	Shallow subtidal
205	Wilmsen *et al.* (2005)	Cenomanian/Essen Greensands, Pläner Limestone, North Germany	Sandstones, siltstones, limestones	Faecal pellets and clays	Near shore to middle shelf (20 m–100 m)
206	Bansal *et al.* (2014); Banerjee *et al.* (2016)	Aptian–Coniacian/Karai Formation	Shales	Foraminifera, ostracoda, bryozoa and algae, faecal pellets, micas	Middle shelf
207	Witts *et al.* (2015)	Maastrichtian/López de Bertodano Formation	Siltstones, sandstones	–	Middle to outer shelf
208	Jiménez-Millán and Castro (2008)	Hauterivian/Los Villares Formation	Sandstones	Feldspars	Middle shelf to slope
209	Isaac *et al.* (1991)	Campanian–Maastrichtian/ Tahora Formation	Sandstones	–	Outer shelf
210	Ostwald (1990)	Cenomanian/Groote Eylandt Mn-deposit, Australia	Sandstones, shales	–	Outer shelf
211	Retzler *et al.* (2013)	Santonian–Campanian/Menuha Formation	Organic-rich chalk	–	Outer shelf
212	Berra *et al.* (2007)	Santonian/Neka Valley, Iran	Limestones	Foraminifera and faecal pellets	Deep marine (200 m–500 m)
213	Ghabeishavi *et al.* (2009)	Coniacian–Santonian/Succession of the Bangestan Palaeo-high in the Bangestan Anticline, Zagros, Iran	Mudstone-wackestone	–	Deep platform
214	El Kadiri *et al.* (2005)	Campanian–Maastrichtian/ Tamezzakht Succession, Morocco	Calcareous sandstones and shales	–	Deep marine
215	Rea *et al.* (1990)	Turonian–Santonian/Indian Ocean, ODP leg 121 (Broken Ridge)	Tuffs	–	Deep marine
216	Roban and Dobrinescu (2012)	Aptian–Albian/Audia Formation, TarcăuNappe, Eastern Carpathians	Sandstones	Faecal pellets	Deep marine turbidite sandstone
217	Afanasjeva *et al.* (2013)	Cenomanian/Melovatskaya Formation, Southeast Russia	Siltstones and sandstones	Faecal pellets	Marine
218	Odin and Matter (1981)	Jurassic–Late Cretaceous/ Unclassified	Sandstones, shales, limestones	Bioclasts, faecal pellets	–
219	Hower (1961); Thompson and Hower (1975)	Jurassic/Sundance Formation	Sandstones	Faecal pellets	–
220	Thompson and Hower (1975)	Jurassic/Weilheim, Germany	–	Faecal pellets	–
221	Misik and Sucha (1994)	Middle–Late Jurassic/Slovak republic	Limestones	Faecal pellets	–
222	Baldermann *et al.* (2012)	Jurassic/Oker, Germany	–	Faecal pellets	Shallow marine/lagoon

(*continued on next page*)

Table 1 – (continued)

Strata No.	Author	Age/Stratigraphic unit, location	Background lithology	Substrate	Environment/ Bathymetry
223	Deconinck and Strasser (1987)	Tithonian–Berriasian/Swiss and French Jura, the northern margin of the Tethys Ocean	Limestones and marls	–	Hypersaline lake, estuary, subtidal, shallow-marine
224	Gygi and Marchand (1982)	Callovian–Oxfordian/Northern Switzerland	–	–	Inner to middle shelf (<100 m)
225	Jiménez-Millán *et al.* (1998)	Jurassic/Zegri Formation, Gavilán Formation; Albian–Turonian/ Represa Formation, Spain	Limestones	Bioclasts	Shelf to slope
226	Hallam and Maynard (1987)	Oxfordian–Valanginian/Chichali Formation	Sandstones	Faecal pellets	Middle shelf
227	Sánchez-Navas *et al.* (1998, 2008); Eder *et al.* (2007)	Jurassic/Georgiev Formation	Claystones, siltstones and limestones	Faecal pellets, alteration of micas or clays	Middle shelf
228	Fürsich (1984)	Late Jurassic/Kap Leslie Formation	Sandstones, siltstones and mudstones	–	Outer shelf
229	Böhm (1986)	Jurassic/Adnet Group, Austria	Limestones	–	Deep marine
230	Strasser *et al.* (2005)	Oxfordian/Ariño Section, Spain	Limestones	Faecal pellets	Deep marine
231	Saraev and Baturina (2008)	Triassic/Bergamak Formation, Yar Formation, Voivov Formation	Sandstones and siltstones	–	–
232	Kirkham (2003)	Triassic/Bristol area, Southwest England	Marly limestones	–	Lacustrine
233	Bozkaya and Yalçin (2013)	Triassic/Yoncali, Uludere and Uzungeçit Formations, Turkey	Limestones	–	–
234	Xie (1991)	Late Triassic/Yanchang Group	Feldspathic sandstones	–	Lacustrine, deltaic
235	El Ghali *et al.* (2009)	Triassic/Grèsá Voltzia and Coquillier Formation	Sandstones, limestones	Alteration of micas	Fluvio-deltaic and shoreface
236	Smalley *et al.* (1986)	Triassic/Barentsøya Formation, Spitsbergen	Sandstones, black shales	Faecal pellets	Marginal marine
237	Vecsei (1998)	Triassic/The southwestern Germanic Basin, Luxemburg	Limestones	–	Tidal flat environment
238	Whiteside and Robinson (1983)	Late Triassic/Limestone at Tytherington Quarry	Sandstones and breccias	Faecal pellets	Brackish environment (~40 m)
239	Parrish *et al.* (2001)	Triassic/Shublik Formation, Arctic Alaska, USA	Sandstones	–	Middle shelf
240	Ketzer *et al.* (2003)	Permian/Rio Bonito Formation, southern Brazil	–	Faecal pellets	Shoreface
241	Cairncross *et al.* (1990)	Permian/Witbank Coalfield, South Africa	Mudstones and siltstones	–	Shallow marine
242	Reid *et al.* (2007)	Permian/Upper Raanes and Great Bear Cape Formations	Limestones, sandstones and siltstones	Bioclasts	Inner to outer ramp (<100 m)
243	Godek and Beauchamp (2011)	Permian/Wordian–Capitanian (Trold Fiord), Sverdrup Basin	Sandstones	–	Inner to outer shelf
244	Dustira *et al.* (2013)	Permian–Triassic/KappStarostin Formation, Svalbard, Norway	Sandstones	–	Outer shelf
245	Thompson and Hower (1975); Morton and Long (1980)	Carboniferous/Barnett Formation, Marble Falls Formation	Shales, limestones	–	–
246	Hower (1961)	Pennsylvanian/Morrow Formation	Sandy shales	Faecal pellets	–
247	Thompson and Hower (1975)	Carboniferous/Canadian Arctic Loc. #3	Sandstones, shales	Faecal pellets	–
248	Wang *et al.* (2011)	Late Carboniferous–Early Permian/ Amushan Formation, Inner Mongolia	Limestones	Faecal pellets	–
249	Hower (1961)	Devonian/Carlisle Cent. Formation	Siltstones	Faecal pellets	–
250	Engalychev and Panova (2011)	Devonian/Arukula Formation, Estonia	Sandstones	–	–
251	Eickmann *et al.* (2009)	Devonian/Pillow basalts of Variscanorogens, Germany	–	–	–

Table 1 – (continued)

Strata No.	Author	Age/Stratigraphic unit, location	Background lithology	Substrate	Environment/ Bathymetry
252	Morton and Long (1980)	Devonian/Stribling Formation, Houy Formation	Shales and limestones	–	–
253	Ball (1941); Foland *et al.* (1984); Grant *et al.* (1984)	Silurian/Brassfield Formation, USA	Limestones	–	–
254	Thompson and Hower (1975); Ershova (2008)	Ordovician/Latorpian Regional Stage	Limestones, sandstones	Bioclasts and faecal pellets	–
255	Egenhoff (2004)	Early Ordovician/Bjørkåsholmen Formation, Norway and Sweden	–	–	–
256	Eriksson *et al.* (2012)	Middle Ordovician/Darriwilian 'Täljsten' interval, Sweden	–	–	–
257	Kim and Lee (2000)	Early Ordovician/Dongjeom Formation, Korea	Sandstones	Alteration of feldspar and mica	Peritidal, shallow marine (5 m–10 m)
258	Lee and Paik (1997)	Ordovician/Mungok Formation, Korea	Limestones	Faecal pellets, alteration of mica	Shallow marine
259	Peters and Gaines (2012)	Ordovician/Au Train Formation	Sandstones	–	Shallow marine
260	Viira *et al.* (2006)	Early Ordovician/Leetse Formation, Toila Formation	Sandstones, limestones	–	Shallow marine
261	Kaya and Friedman (1997)	Ordovician/Antelope Valley Limestone, USA	Lime mudstones	Faecal pellets	Middle shelf
262	Odin and Matter (1981); Odin and Fullagar (1988)	Ordovician/Estonia	Sandstones, shales, limestones	Bioclasts, faecal pellets, alteration of micas, quartz, chert and feldspars	–
263	Hower (1961)	Ordovician/Tyner Formation, Seratopyge sandstone	Limestone	Faecal pellets	–
264	Hower (1961); Thompson and Hower (1975)	Cambrian/Tonto Formation, Mt. Whyte Formation, GrosVentre Formation, Murray Shale	Sandstones, shales	Faecal pellets	–
265	Ball (1941); Hower (1961); Foland *et al.* (1984), Grant *et al.* (1984)	Late Cambrian/Bonneterre Formation, Davis Formation	Limestones	–	–
266	Gomez and Astini (2015)	Early–Middle Cambrian/Soldano and Juan Pobre Members, Argentine Precordillera	–	–	–
267	Ivanovskaya and Geptner (2004)	Early Cambrian/Virbalis Formation	Sandstones, siltstones mudstones	Alteration of mica and quartz	–
268	Baqri *et al.* (1994)	Cambrian/Kussak Formation	Shales and sandstones	–	–
269	Brasier (1980)	Cambrian/Forteau Formation, Fucoid beds (Northweat Scotland), Bastion Formation, Lancara/ Vegadeo Formation, Pedroche Formation, Carterat Grey Schist (Normandy), Comley Formation, Home Farm and Wood members (Warwickshire)	Shales, sandstones, limestones	–	–
270	Hower (1961); Chafetz (1978); Morton and Long (1980); Chafetz and Reid (2000); Chafetz (2007); Cecil and Ducea (2011)	Cambro-Ordovician/Riley Formation, Wilberns Formation	Sandstones	Faecal pellets	Shallow marine (<10 m)
271	Hower (1961); Odom (1976); Rolf *et al.* (1977)	Cambrian/Deadwood Formation, Franconia Formation, USA	Sandstones	Faecal pellets	Near shore, shallow water environment

(*continued on next page*)

Table 1 – (continued)

Strata No.	Author	Age/Stratigraphic unit, location	Background lithology	Substrate	Environment/ Bathymetry
272	Berg-Madsen (1983)	Cambrian/*Acrothelegranulata* Conglomerate of Sweden and *Exsulans* Limestone Formation	Siltstones and limestones	Bioclasts	Shallow marine (<50 m)
273	Chen *et al.* (1988)	Cambrian–Ordovician/ Unclassified, Xiaoyangqiao, Jilin Province	Sandstones	–	Shallow marine
274	Korkutis (1981)	Cambrian/Lontova Formation	Sandstones	–	Shallow marine
275	Long and Yip (2009)	Cambrian/Bradore Formation	Sandstones	–	Shallow shelf
276	Eoff (2014)	Cambrian/Lone Rock and Mazomanie Formation	Sandstones	–	Inner to middle shelf
277	Kordi *et al.* (2011)	Cambrian–Ordovician/Lower sandstone unit in southwestern Sinai, Egypt	Sandstones	Faecal pellets, micas and feldspar	Subtidal
278	Longuépée and Cousineau (2006)	Cambrian/AnseMaranda Formation	Sandstones	Faecal pellets	Middle to outer shelf
279	Li *et al.* (1996)	Neoproterozoic/Jingeryu Formation	–	–	–
280	Lo (1980)	Late Proterozoic–Early Phanerozoic/Pestrotsvel Formation	Limestones	–	–
281	Zaitseva *et al.* (2000)	Late Riphean (800–100 Ma)/UK Formation, Russia	Sandstones and silstones	–	–
282	Ivanovskaya *et al.* (2006); Ivanovskaya *et al.* (2014)	Middle Riphean (1300–1100 Ma)/ Arymas Formation, Khaipakh Formation, Russia	Sandstones, siltstones	–	–
283	Ivanovskaya *et al.* (2012)	Late Proterozoic/Anabar and Olenak uplifts, Siberia	Sandstones	Alteration of clay mineral	–
284	Anderson *et al.* (2013)	Neoproterozoic/Bonahaven Formation, Scotland	Sandstones	–	Tidal flat
285	Dasgupta *et al.* (1990)	Middle Proterozoic/Ramgiri Formation, Ramagundam Sandstone; Paleoproterozoic/ Pandikunta Limestone	Sandstones	–	Intertidal shoal bar, estuarine, fluvial
286	Drits *et al.* (2010)	Paleoproterozoic/Yusmastakh Formation, Anabar Uplift	Impure dolomites	–	Shallow marine
287	Singh and Kumar (1978); Banerjee *et al.* (2008)	Paleoproterozoic/Kheinjua Formation, Deoland Formation, Chitrakut Formation, Semri Group	Sandstones	–	Inner shelf
288	Day *et al.* (2004)	Neoproterozoic/Keele Formation, Mackenzie Mountains, Canada	Sandstones and siltstones	–	Shallow marine
289	Reynolds (1963)	Late Proterozoic/Northern Rocky Mountains	Impure limestones	–	Shallow marine
290	Guimaraes *et al.* (2000)	Neoproterozoic/Paranoa Group, Brazil	Sandstones	–	Shallow marine
291	Sarkar *et al.* (2014)	Neoproterozoic/Bhander Limestone, Vindhyan Basin	Impure limestones	–	Shallow marine
292	Kale and Peshwa (1995)	Neoproterozoic/Rabanpali Formation	Sandstones	–	Shallow marine
293	Gulbrandsen *et al.* (1963)	Mesoproterozoic/Belt Series, Montana, USA	Sandstones	–	Shallow marine
294	Guimaraes *et al.* (2000)	Mesoproterozoic/Paranoa Group, Brazil	Sandstones	–	Shallow marine
295	Rawlley (1994)	Mesoproterozoic/Rewa Group	Sandstones	Feldspar	Shallow marine
296	Bhattacharyya *et al.* (1986)	Paleoproterozoic/Semri Formation	Dolomites	–	Shallow marine
297	Richards and Gee (1985)	Paleoproterozoic/Yelma Formation and Wandiwarra member of Chiall Formation	Dolomites and sandstones	–	Shallow marine
298	Xu (2010)	Paleoproterozoic/Majiahe Formation, North China Craton	Sandstones	–	Shallow marine
299	Misi *et al.* (2014)	Neoproterozoic/Rocinha Formation, Vazante Group, Brazil	Sandstones	–	Marine

Table 1 — (*continued*)

Strata No.	Author	Age/Stratigraphic unit, location	Background lithology	Substrate	Environment/ Bathymetry
300	Conrad *et al.* (2011)	Mesoproterozoic/1. Chanda Limestone, 2. Raipur Group, Chattsigarh Basin, 3. Chandarpur Group, India; Paleoproteropzoic/4. Somanpalli Group, India	Sandstones	Feldspar	Deep marine (1); Shallow marine (2, 3, 4)
301	Meng (2006); Mei *et al.* (2008); Zhou *et al.* (2009)	Mesoproterozoic/Tieling Formation, China	Impure limestones	—	Subtidal, intertidal flat
302	Deb and Fukuoka (1998); Bandopadhyay (2007)	Neoproterozoic/Penganga Group, India	Sandstones	—	Deep marine

Note: This table is arranged as per the age of glaucony record and for the same age environmental interpretations from shallow to deep are considered. If a same author has reported glaucony from multiple stratigraphic levels, each level has been considered for a separate record.

sedimentation breaks to mega-condensed sections (Amorosi, 2012; and references therein), the records of glaucony occurrence through geological time are poorly known, and temporal variation in glaucony composition has never been addressed. The occurrence of modern glaucony in deeper shelf and slope regions is frequently extrapolated to interpret the depositional settings of ancient glaucony-bearing sedimentary sequences. However, the ancient varieties of glaucony occur in wide ranging palaeo-depositional conditions. Although a few researchers have attempted to relate the glaucony composition with the depositional environment, factors affecting the glaucony composition are poorly understood.

McRae (1972) and Odin and Matter (1981) presented an exhaustive discussion regarding the origin of glaucony and its morphological, mineralogical and chemical variations. This paper presents an up-to-date review regarding the following aspects: (1) depositional significance of glaucony, (2) abundance of glaucony through geological time, (3) temporal variation of glaucony composition through time, particularly focusing on the compositional difference between the Precambrian and the Phanerozoic glaucony, and (4) influence of the depositional environment and the substrate on the composition of glaucony.

2. Nomenclature, mineralogy and chemical variations in glaucony

Glauconite is a potassium- and iron-rich dioctahedral sheet silicate with the general formula of $(K,Na,Ca)(Fe,Al,Mg,Mn)_2(Si,Al)_4O_{10}(OH)_2$. Odin and Létolle (1980) proposed the term 'glaucony' to include the wide ranging chemical composition of sand-sized, green grains irrespective of their mineralogical affinity. Subsequently, Odin and Matter (1981) introduced the term 'glauconitic minerals' for high-Fe glaucony (>15% total Fe_2O_3 (TFe_2O_3)) with glauconitic smectite (3%–5% K_2O) and glauconitic mica (>5% K_2O) as end members; progressive incorporation of K_2O in the glaucony structure converts the former 'immature' variety into the latter 'mature' variety. They also considered a compositional gap between illitic minerals (<10% TFe_2O_3) and glauconitic minerals (>15% TFe_2O_3) between 10% and 15% TFe_2O_3. Later researchers, however, reported a compositional continuum between these two end members (Kossovskaya and Drits, 1970; Berg-Madsen, 1983; Ireland *et al.*, 1983; Dasgupta *et al.*, 1990; Deb and Fukuoka, 1998).

In this paper, unless specified, glauconitic smectite, glauconitic mica as well as ferric illite are considered as 'glaucony'. Glaucony exhibits the basal reflection (001) located between 14 Å and 10 Å (Odin and Matter, 1981) that sharpens upon glycolation and heating; other peaks may include (020) at 4.53 Å, (003) at 3.33 Å, $11\bar{2}$, 112 and (060) at 1.51 Å. The unit structure of ordered glauconite mica is characterized by 10% expandable layer, high K content, 1 M stacking sequence and well-defined $11\bar{2}$ and 112 reflections. The 00L reflections at 10.1 Å, 4.53 Å and 3.3 Å are symmetrical and sharp (Burst, 1958a; Hower, 1961; Wermunde, 1961; Bentor and Kastner, 1965; McRae, 1972; Odin and Matter, 1981; Odom, 1984). Upon glycol solvation, the (001) peak remains unmoved (Odin and Matter, 1981). The peak at 10 Å is sharp while other peaks show a broad base with asymmetrical sides. The glauconitic smectite contains the lowest K content and the structure is extremely disordered. The glauconite and smectite layers are usually randomly interstratified. AIPEA (Association Internationale Pour I'Étude des Argiles) defined glauconite as a dioctahedral mica with tetrahedral Al^{3+} (or Fe^{3+}) > 0.2 atoms per formula unit, octahedral R^{3+} > 1.2 atoms (Bailey, 1980). Fe occurs in both ferrous and ferric state. Fe^{2+} usually comprises about 5%–12% of the total iron. Glauconite is distinguished from celadonite by its higher octahedral charge and higher levels of the substitution of aluminium for silicon in the tetrahedral layer (Duplay and Buatier, 1990). Glauconite, Fe-illite and Fe–Al-smectites form contiguous compositional domains and therefore it is difficult to distinguish these minerals on the basis of major element composition alone. Meunier and El Albani (2007) considered an interlayer charge to distinguish different types of iron silicate minerals. Compositional domains of iron-bearing phases, namely glaucony, Fe-illites and Fe–Al-smectites are distinguished on the basis of $M^+/4Si$ *vs.* Fe/Sum of octahedral cations; M^+ corresponds to interlayer charge (Na + K + 2Ca). However, the definition of glauconitic minerals provided by Bailey (1980) includes a wider compositional range in glaucony compared to the definition proposed by Meunier and El Albani (2007). Many of the glaucony data reported in Banerjee *et al.* (2008, 2012a, 2012b) do not plot in the glaucony field of Meunier and El Albani (2007), although they satisfy the definition of Bailey (1980).

Glaucony is characterized mainly on the basis of the K_2O–Fe_2O_3 relationship. The K_2O content of glaucony is a measure of its evolution; four types of glaucony are distinguished, nascent (2%–4% K_2O), slightly evolved (4%–6% K_2O), evolved (6%–8% K_2O) and highly evolved (>8% K_2O) (Odin and Matter, 1981; Amorosi, 1997, 2012). The level of maturity (evolution) reached by glauconitic mineral depends on the residence time of grains close to the sediment–water interface, and hence the sedimentation rate is important. The residence time of highly evolved glaucony grains is estimated to be 10^5–10^6 years and therefore these are generally considered as a proxy for significant breaks in deposition (McRae, 1972; Odin and Matter, 1981; Odin and Fullagar, 1988; Amorosi, 2012). The color of glaucony is reported to be darker during the course of maturation (see Amorosi, 1997, 2012 and references therein). However, the exact reasons related to this change in color of glaucony with variation in K_2O are yet to be explored from a crystallographic point of view. The predominant Al–Fe substitution in the octahedral site is reported by many researchers (Odin and Matter, 1981; Bornhold and Giresse, 1985; Velde, 1985; Dasgupta *et al.*, 1990; Amorosi *et al.*, 2007; Eder *et al.*, 2007; Banerjee *et al.*, 2008, 2012a, 2012b, 2015; Chang *et al.*, 2008; Sánchez-Navas *et al.*, 2008).

3. Palaeogeographic implications of glaucony

Odin and Matter (1981) found that glaucony is widespread in the depth range of 50 m–500 m in modern seas and are most common at around 200 m–300 m of depth. The same bathymetric interpretation is usually extrapolated for ancient glaucony. However, the ancient varieties are reported from wide ranging depositional conditions from shallow marine to deep marine (Morton *et al.*, 1984; Baldermann *et al.*, 2012), through lagoons (El Albani *et al.*, 2005; Banerjee *et al.*, 2012a), estuaries and tidal flats (Dasgupta *et al.*, 1990; Huggett and Gale, 1997; Chafetz and Reid, 2000), inner to outer shelf (Garzanti *et al.*, 1998; Kelly and Webb, 1999; Kelly *et al.*, 2001; Banerjee *et al.*, 2008, 2012b, 2016; Chattoraj *et al.*, 2009) and even in continental environments in rare cases (Table 1; Fig. 1). Glaucony is reported from lacustrine/palaeosol sediments in rare cases (Kirkham, 2003; Huggett and Cuadros, 2010). The maximum depth of authigenic glaucony is reported from 2500 m (Morton *et al.*, 1984) in a Middle Miocene calcareous ooze deposit in the North Atlantic Ocean. Amorosi (1997) considered that most outer-shelf-originated glaucony are of autochthonous nature, while those formed in shallow marine and deep marine conditions are of para-autochthonous and detrital varieties. However, ancient autochthonous glaucony has been reported from both the shallow marine (Dasgupta *et al.*, 1990; Chafetz and Reid, 2000; El Albani *et al.*, 2005; Banerjee *et al.*, 2008, 2015) and the deep marine settings (Morton *et al.*, 1984; Giresse and Wiewióra, 2001; Baldermann *et al.*, 2013). Our study, including both modern and ancient glaucony occurrences indicates that the most ancient variety formed in inner to outer shelf depositional settings. Shelf-originated glaucony comprises around ~71% of the total record. The deep marine depositional setting, beyond the shelf-break accounts for ~10% of glaucony occurrences, most of which are found within modern to Pliocene ages. The non-availability of Fe in deep basinal seawater may be one of the main reasons for the paucity of glaucony in the deep marine environment. Our study indicates that a shelf environment is the favourable site for the formation of glaucony (Fig. 1). Porrenga (1967) reported the abundance of glaucony in the modern ocean at a depth interval 125 m–500 m, where the annual temperature was between 10 °C and 15 °C. The paucity of glaucony at a water depth greater than 500 m in tropical seas and its complete absence in Arctic and Antarctic Seas suggests significant temperature control in its formation (Porrenga, 1967). Bjerkli and Östmo-Saeter (1973), nevertheless, reported glaucony from water temperatures as low as 6 °C, corresponding to a depth of 250 m. Modern deep marine conditions (>1000 m depth) and a low temperature of <6 °C appear to be unusual conditions for glaucony formation (Buatier *et al.*, 1989; Giresse and Wiewióra, 2001; Gaudin *et al.*, 2005; Cuadros *et al.*, 2011; Baldermann *et al.*, 2013). A cold environment is unfavourable for glaucony formation possibly because of a combination of factors such as a limited supply of silicates, low reaction rates and less microbial activity (Schulz and Zabel, 2006; Baldermann *et al.*, 2013). The rate of glauconitization appears to be about five times slower in the deep marine environment (>1000 m) compared to shallow shelf regions (Baldermann *et al.*, 2013).

4. Records of glaucony in geological time in relation to sea level and climate

Van Houten and Purucker (1984) indicated that the geological records of glaucony depended on a global rise and fall of sea level. 453 occurrences of glaucony from modern and ancient sedimentary records roughly correspond to the first- and second-order sea-level curves of Vail *et al.* (1977) (Table 1; Fig. 2). However, Quaternary, Neogene, Paleogene and Cretaceous, the last four Periods of Earth's history, record the majority (~73%) of glaucony occurrences. These records roughly correspond to a high sea level and a greenhouse climate. The oldest glaucony possibly belongs to the Late Paleoproterozoic time (Basu and Bickford, 2014). The absence of glaucony in the Early Paleoproterozoic and the Archaean rocks is possibly related to its alteration to chlorite. Glaucony occurring in the Mesoproterozoic Arymas Formation in the Siberian Basin exhibits frequent alteration to chlorite (Ivanovskaya *et al.*, 2006). The Cambrian was possibly the most favourable time for the formation of glaucony during the entire Paleozoic (Fig. 2). Glaucony is rare in the Late Ordovician, Early Silurian and Late Devonian which corresponds to widespread glacial events. The abundance of glaucony thus coincides well with the second-order sea-level rise in the Paleozoic (Fig. 2). Approximately 29% of the total glaucony record occurs within the Cretaceous. The high sea level corresponding to warm

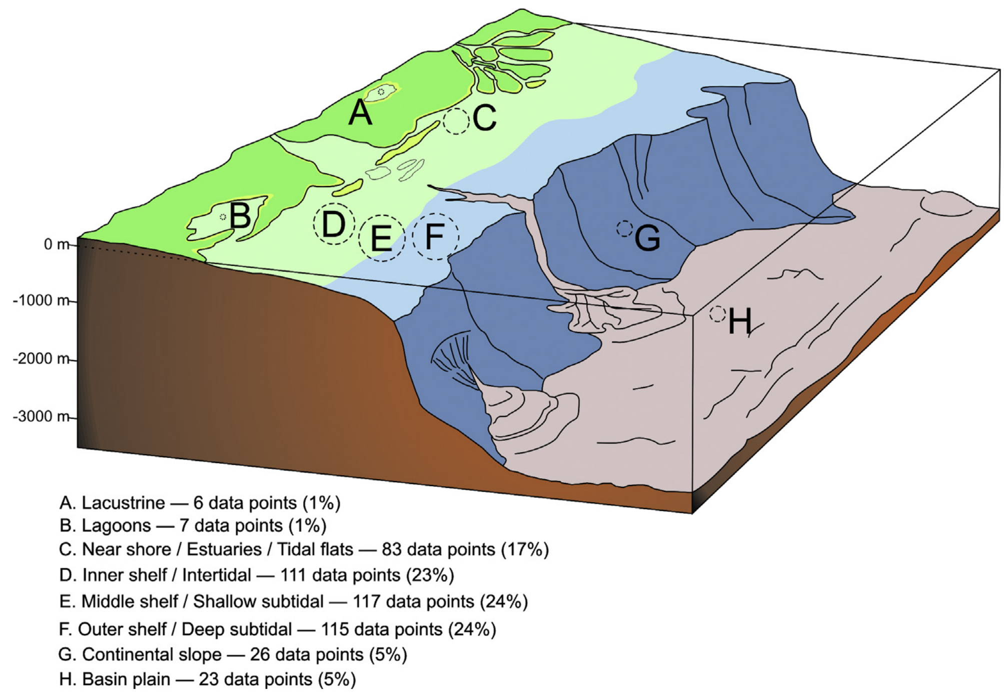

Fig. 1 – Glaucony occurrences (including both modern and ancient ones) in different depositional environments. Note paucity of glauconite beyond the shelf edge. (the figure is modified after Nichols, 2012)

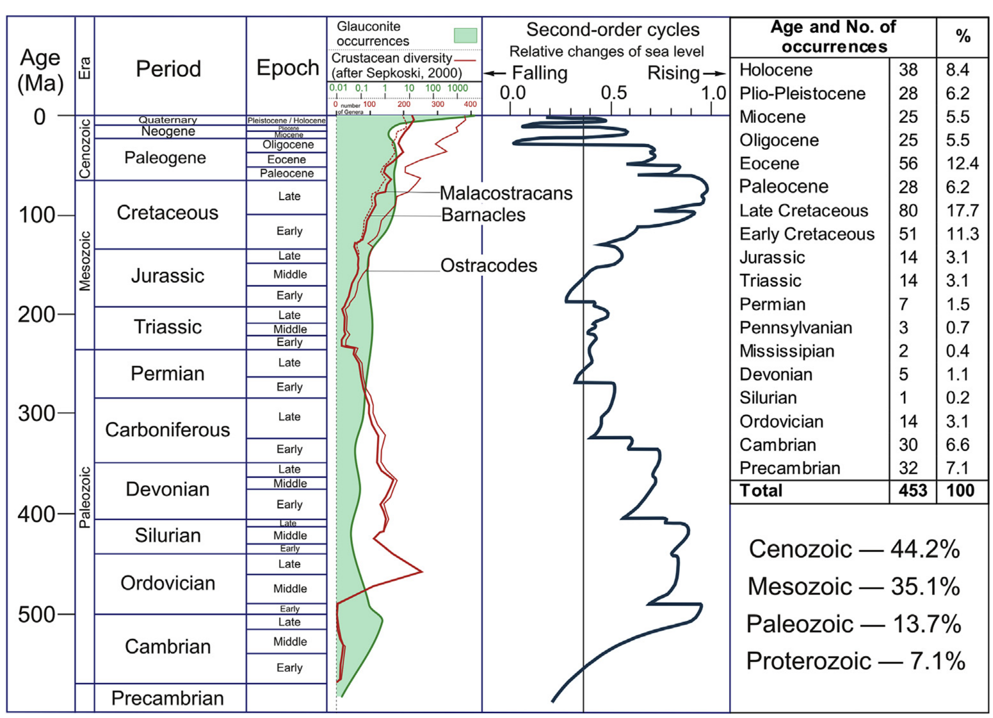

Fig. 2 – Glaucony occurrences through geological time compared with the sea level curve and Crustacean diversification chart. Glaucony occurrences for each time interval are provided in the log scale (marked in green); actual number of occurrences in different intervals is divided by their time duration. Number of Crustacean genera is provided in red (after Sepkoski, 2000). The actual number of glaucony occurrences for each time interval is provided in the table at the right of the figure.

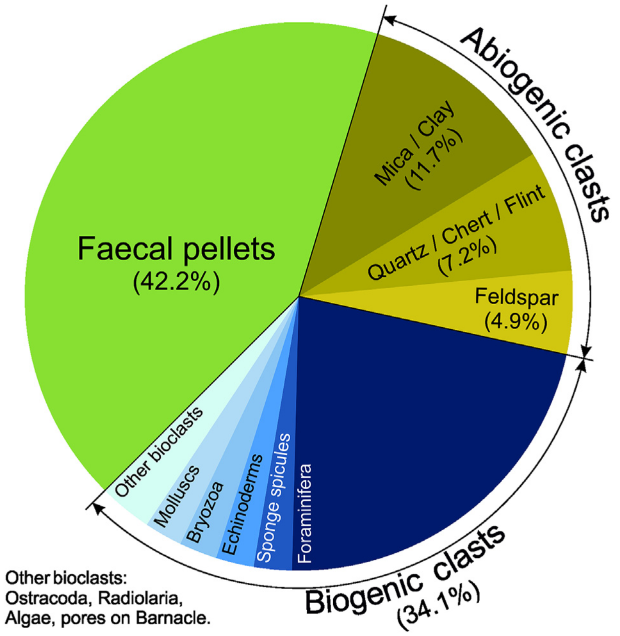

Fig. 3 – Pie chart showing relative contribution of different substrates in the formation of glaucony.

conditions was favourable for glaucony formation during the Cretaceous. The Cenozoic accounts for approximately 42% glaucony record and the peak in glaucony formation took place during the Eocene (~12.4% of total record), which represents a high sea level and warm seawater. A fall in glaucony abundance is noticed at the end of the Eocene that witnessed a sharp fall in the sea level and advent of cold climate. Stassen *et al.* (2012) and Sluijs *et al.* (2014) reported a close association of glaucony with the Paleocene–Eocene Thermal Maxima (PETM), which is considered as one of the warmest times in ocean waters across the globe (Zachos *et al.*, 2006; and references therein).

5. Influence of substrate on abundance of glaucony

The sharp rise of glaucony records from the Cretaceous onward and the highest abundance of glaucony during the Cenozoic are possibly related to the availability of suitable substrates. Faecal pellets and bioclasts are the most favourable substrates for glaucony formation, which together comprise more than 76% of the record (Fig. 3). These organic-rich, sand-sized porous substrates are ideal for the formation of glaucony pellets. The reducing micro-environment within them facilitates glaucony formation by mobilizing iron from background sediments (Meunier and El Albani, 2007; Baldermann *et al.*, 2012; Banerjee *et al.*, 2012a, 2012b). They are available in a broad range of depositional conditions from shallow to deep marine. Crustacean and gastropod faecal pellets predominate on the modern sea floor. Crustaceans have experienced tremendous diversification after the Jurassic as a huge number of genera of barnacles and Malacostracans were added (Fig. 2; Sepkoski, 2000). Gastropoda blossomed during the Middle–Late Cretaceous, and many genera and families of Cenozoic gastropoda, particularly of Neogastropoda appeared during the Late Cretaceous. Similarly, planktonic Foraminiferidae expanded markedly in the Early- to Mid-Cretaceous (Hart, 1999), which is possibly related to an increased delivery of nutrients, including dissolved iron and greater oceanic productivity (Erba, 1994; Erbacher *et al.*, 1996; Leckie *et al.*, 2002). Biotic evolution since the Cretaceous, therefore accounts for ~71% of the glauconite record.

Abiogenic substrates including mica, feldspar and quartz comprise up to 24% of the total glaucony record. Precambrian glaucony formed exclusively within the sand-sized, abiogenic substrates (Deb and Fukuoka, 1998; Dasgupta *et al.*, 1990; Bandopadhyay, 2007; Banerjee *et al.*, 2008, 2015; Ivanovskaya *et al.*, 2012). The Precambrian glaucony thus might have a completely different pathway of evolution than that of Phanerozoic glaucony.

6. Temporal variation in glaucony composition

Fig. 4 exhibits variations in TFe_2O_3 (total), Al_2O_3 and K_2O content of glaucony through time. The TFe_2O_3 content of all Precambrian glaucony is considerably less than the Phanerozoic glaucony. In the case of Precambrian glaucony the TFe_2O_3 content is always less than 20% while Mesozoic and Cenozoic glaucony mostly contains more than 20% TFe_2O_3 (Fig. 4). The inverse relationship between TFe_2O_3 and Al_2O_3 is reported in many works (Odin and Matter, 1981; Bornhold and Giresse, 1985; Velde, 1985; Dasgupta *et al.*, 1990; Amorosi *et al.*, 2007; Eder *et al.*, 2007; Banerjee *et al.*, 2008, 2012a, 2012b, 2015, 2016; Chang *et al.*, 2008; Sánchez-Navas *et al.*, 2008). Because of the low TFe_2O_3 of Precambrian and Paleozoic glaucony, its Al_2O_3 content is appreciably higher than Mesozoic and Cenozoic glaucony (Fig. 4). The K_2O content is usually high in most Precambrian glaucony, including both nascent and

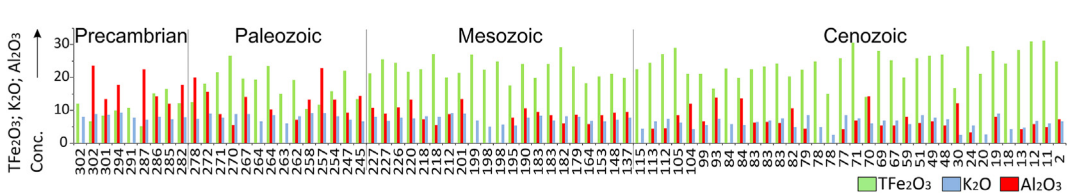

Fig. 4 – Bar diagram showing variation in TFe_2O_3 (total), K_2O and Al_2O_3 content in glaucony through geological time. Note increase in TFe_2O_3 and decrease in Al_2O_3 in younger glaucony. The number corresponds to the serial number mentioned in Table 1.

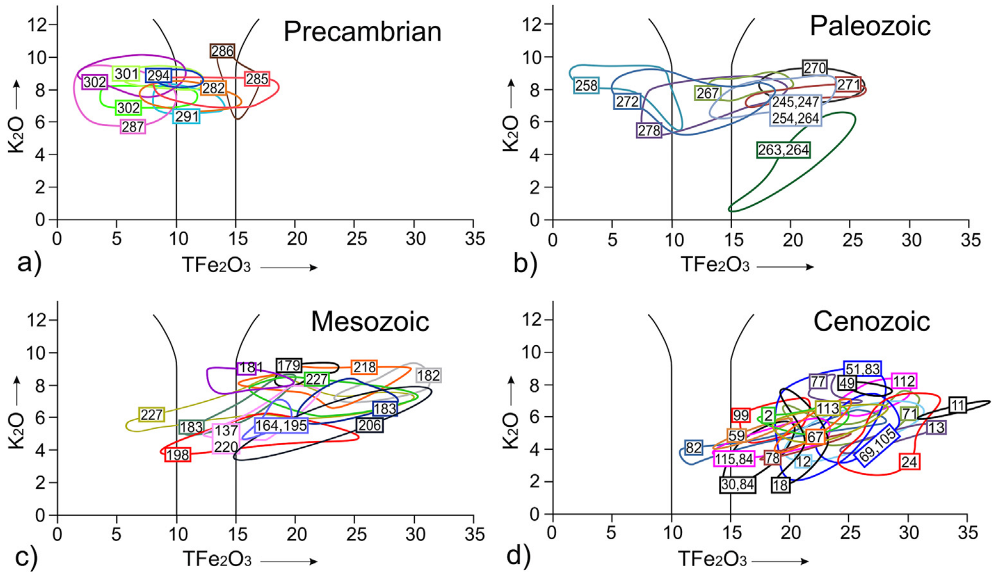

Fig. 5 – K_2O *vs.* TFe_2O_3 (total) relationship in glaucony through geological time. The number in the K_2O–TFe_2O_3 field of glaucony corresponds to the serial number mentioned in Table 1. TFe_2O_3 values between 10% and 15% were considered as a compositional gap by Odin and Matter (1981), separating illitic minerals from glauconitic minerals.

highly evolved varieties, while it is highly variable in Phanerozoic glaucony. The high K_2O content (>8%) in Mesozoic and Cenozoic glaucony is related to a significant stratigraphic condensation (Amorosi, 2012).

The K_2O *vs.* TFe_2O_3 relationship of glaucony exhibits considerable variation over geological time as revealed in Fig. 5. Three types of evolutionary trends are commonly envisaged in glaucony which are as follows.

1) Transformation of degraded layer lattice structures by synchronous fixation of K and Fe ('layer lattice theory'; Burst, 1958a, 1958b; Hower, 1961). A good positive correlation between K_2O and TFe_2O_3 in many examples prompts this theory (Hower, 1961; Bornhold and Giresse, 1985; Eder *et al.*, 2007; Sánchez-Navas *et al.*, 2008; Banerjee *et al.*, 2012a). This trend dominates in Mesozoic and Cenozoic glaucony.
2) Increase in the K_2O content of glaucony at a more or less constant TFe_2O_3 content ('verdissement theory'; Odin and Matter, 1981). As per 'the verdissement theory' glauconitic smectite initially precipitates within the tiny pore spaces in bioclasts and faecal pellets, which is followed by dissolution and recrystallization of the substrate by the addition of K_2O into the glaucony structure without the increase of TFe_2O_3 (Odin and Matter, 1981). Although the verdissement theory is well publicized (Odin and Matter, 1981; Amouric and Parron, 1985; Amorosi, 1995, 2012; Huggett and Gale, 1997; Kelly and Webb, 1999), this trend is poorly represented in Mesozoic and Cenozoic glaucony.
3) Dissolution and replacement of the original substrate, no matter whether it is porous or non-porous ('pseudomorphic replacement theory'; Dasgupta *et al.*, 1990). The constant K_2O content with highly variable TFe_2O_3 in many examples prompted this theory (Dasgupta *et al.*, 1990; Deb and Fukuoka, 1998; Banerjee *et al.*, 2008, 2015).

Even a cursory look at Fig. 5 reveals that all Precambrian glaucony evolved following the third trend and their origin may be explained by the 'pseudomorphic replacement' theory and in contrast Mesozoic and Cenozoic depicts predominantly the first trend; the second and the third trends are insignificant. However, in many examples supporting the 'layer lattice theory', the high content of K_2O (>5%) as well as the TFe_2O_3 (>15%), in the least evolved glaucony do not comply well with layer lattice silicates. In such cases, a model combining initial authigenic precipitation of K-poor glaucony, followed by incorporation of both Fe and K during the later stages of maturation, explains the formation of glaucony (Banerjee *et al.*, 2012a, 2012b, 2016). The Paleozoic glaucony, in this background, presents a mixture of the first and third trends.

7. Distinction between Precambrian and Phanerozoic glaucony

Precambrian glaucony is distinguished from its Phanerozoic counterpart in the following aspects.

1) Precambrian glaucony is characterized by high K_2O, Al_2O_3 and MgO and low Fe_2O_3 contents, which is common in Precambrian occurrences (Figs. 4 and 5). The high MgO content of Precambrian glaucony is possibly related to the high Mg content of Precambrian seas (Banerjee *et al.*, 2008). The interpretation is valid for arkosic or sub-arkosic sandstones, which are devoid of ferro-magnesium minerals.

2) Maturation of glaucony takes place by the addition of TFe_2O_3 at a constant value of K_2O. Even for the incipient glaucony, K_2O content remains high (Dasgupta *et al*., 1990; Deb and Fukuoka, 1998; Banerjee *et al*., 2008, 2015).
3) Authigenic glaucony pellets usually formed in shallow marine environments in the Precambrian because of availability of sandy sediments. Most Precambrian glaucony are, therefore, reported from sandstones, while the bulk of the Phanerozoic authigenic glaucony are found in shales.
4) The TFe_2O_3 content of Precambrian glaucony is less. The high TFe_2O_3 content of Phanerozoic glaucony is possibly related to a combination of continental weathering, upwelling and submarine volcanism, which caused the elevation of Fe content in the seawater. Fe is also mobilized as the degradation of organic matter creates a reducing micro-environment within the substrate. In the case of Precambrian glaucony, mobilization of iron from the substrate is totally excluded. Fe in shallow marine sands is possibly supplied mostly from continental weathering.
5) The high K_2O content of Precambrian glaucony is possibly related to the K-feldspar substrate. Precambrian glaucony is always rich in potassium irrespective of its degree of evolution, while the high K content in Phanerozoic-evolved glaucony indicates significant stratigraphic condensation. A shallow marine-originated arkosic to sub-arkosic sandstone appears to be the most favourable host rock.

8. Variation of glauconite composition in relation to substrate and depositional conditions

There has been a consensus that while ferric illite is a typical product in high salinity lacustrine and lagoonal environments (Parry and Reeves, 1966; Porrenga, 1968; Kossovskaya and Drits, 1970), whereas true glaucony of Odin and Matter (1981) belongs to continental shelf and outer slope at water depths between 50 m and 500 m. Crystallo-chemical properties of glaucony may then be sensitive to local physico-chemical conditions of its depositional environment (El Albani *et al*., 2005). The following aspects lend support to this conclusion.

Incorporation of large amount of Fe ions into the glaucony structure is favoured in a reducing and acidic environment that may be created by the decomposition of organic matter. Consequently, pyrite is a common associate of glaucony (Kelly and Webb, 1999; Lee *et al*., 2002; El Albani *et al*., 2005). Had the depositional environment been oxic, mobility of Fe ions would be restricted, starving the authigenic mineral in Fe; goethite may be associated in this case. Freshwater input decreases K^+ ion activity and makes the authigenic glaucony K-poor, Fe-poor and Al-rich, forming at a depth of 0 m–10 m (Berg-Madsen, 1983; El Albani *et al*., 2005).

Alternatively glaucony composition is dependent on its substrate (Dasgupta *et al*., 1990; Banerjee *et al*., 2008, 2015, 2016). Banerjee *et al*. (2012a, 2012b) showed that the Fe and K content of glaucony varies considerably, depending on the porosity and permeability characteristics of the substrate; Cenozoic glaucony formed within faecal pellets were considerably richer in Fe and K compared to those in the tiny pore spaces of benthic foraminifers.

9. Conclusions

A review on glaucony highlights some of the crucial aspects related to its palaeogeographic implications and temporal variation.

1) Most Phanerozoic glaucony originated in a shelf setting. Warm seawater and high eustatic sea level facilitated glaucony formation, while deep marine conditions and low seawater temperature were unfavourable for glaucony formation. Because of the availability of suitable substrates such as faecal pellets and bioclasts, the Cretaceous to the Holocene glaucony comprises 75% of the total record.
2) TFe_2O_3 (total), Al_2O_3, K_2O and MgO content of glaucony varied through geological time. While TFe_2O_3 content of most Mesozoic and Cenozoic glaucony exceeded 20%, in the case of Precambrian glaucony it remained always less than 20%.
3) K_2O *vs*. TFe_2O_3 relationship of glaucony exhibits considerable variation over geological time. Three types of evolutionary trends correspond to three popular models regarding glaucony formation, namely, 'layer lattice theory', 'verdissement theory' and 'pseudomorphic replacement theory'. The first two theories explain the origin of most Phanerozoic glaucony, while most Precambrian glauconite indicates 'pseudomorphic replacement' of the substrate.
4) The composition of the substrate and depositional conditions influenced glaucony composition significantly. Glaucony formed within K-feldspar substrate, either poorly or highly evolved, is rich in potassium. Faecal pellets are found to be the most favourable substrate for the evolution of glaucony. Slightly reducing conditions favour the origin of high-Fe glaucony. Glaucony formed in oxidising conditions are depleted in Fe. Influx of freshwater into the depositional setting may cause depletion of potassium in the glaucony structure.
5) Precambrian glaucony is distinguished from its Phanerozoic counterpart by its high K_2O, Al_2O_3, MgO and low TFe_2O_3 content. Even the least evolved glaucony contains high potassium values (7%–9%). Similar high values in the case of Phanerozoic glaucony are believed to represent significant stratigraphic condensation. Evolution of Precambrian glaucony took place by the addition of TFe_2O_3 at a constant K_2O. Precambrian glaucony formed in shallow marine depositional conditions, mostly within the shoreface region, because of the availability of sand-size substrates. In contrast, Phanerozoic glaucony mostly formed in the middle to outer shelf depositional conditions. These glaucony varieties formed within shallow marine-originated arkosic to sub-arkosic sandstones containing K-feldspar.

Acknowledgements

The authors are indebted to their host institutes for infrastructure facilities. Santanu Banerjee is thankful to Department of Science and Technology, Government of India for financial support through Grant IR/S4/ESF-16/2009(2). Authors are thankful to DST-IITB National Facility for EPMA, Department of Earth Sciences, Indian Institute of Technology Bombay. The authors are thankful to P.G. Eriksson and Ian D. Somerville for their constructive criticisms and useful suggestions on earlier version of the manuscript.

REFERENCES

Afanasjeva, N.I., Zorina, S.O., Gubaidullina, A.M., Naumkina, N.I., Suchkova, G.G., 2013. Crystal chemistry and genesis of glauconite from "Melovatka" section (Cenomanian, of South-Eastern Russian Plate). *Litosfera* 2, 65–75.

Ahmad, F., Farouk, S., Abd El-Moghny, M.W., 2014. A regional stratigraphic correlation for the upper Campanian phosphorites and associated rocks in Egypt and Jordan. *Proceedings of the Geologists' Association* 125, 419–431.

Aitchison, J.C., 1988. An Eocene storm-generated littoral placer, Northeast Otago, New Zealand. *Journal of Geology and Geophysics* 31 (3), 381–383.

Altaner, S., Demosthenous, C., Pozzuoli, A., Rolandi, G., 2013. Alteration history of Mount Epomeo Green Tuff and a related polymictic breccia, Ischia Island, Italy: evidence for debris avalanche. *Bulletin of Volcanology* 75, 718.

Amaral, G., 1967. Potassium-argon age measurements on some Brazilian glauconites. *Earth and Planetary Science Letters* 3, 190–192.

Amireh, B.S., 1997. Sedimentology and palaeogeography of the regressive–transgressive Kurnub Group (Early Cretaceous) of Jordan. *Sedimentary Geology* 112, 69–88.

Amireh, B.S., Jarrar, Gh., Henjes-Kunst, F., Schneider, W., 1998. K-Ar dating, X-ray diffractometry, optical and scanning electron microscopy of glauconies from the Early Cretaceous Kurnub Group of Jordan. *Geological Journal* 33, 49–65.

Amorosi, A., 1994. The glaucony-bearing horizon of the Lower Miocene Bisciaro Formation (Umbria–Marche Apennines). *Giornale di Geologia* 56, 7–16.

Amorosi, A., 1995. Glaucony and sequence stratigraphy: a conceptual framework of distribution in siliciclastic sequences. *Journal of Sedimentary Research* 65, 419–425.

Amorosi, A., 1997. Detecting compositional, spatial, and temporal attributes of glaucony: a tool for provenance research. *Sedimentary Geology* 109, 135–153.

Amorosi, A., 2011. The problem of glaucony from the Shannon Sandstone (Campanian Wyoming). *Terra Nova* 23, 100–107.

Amorosi, A., 2012. The occurrence of glaucony in the stratigraphic record: distribution patterns and sequence–stratigraphic significance. *International Association of Sedimentologists Special Publications* 45, 37–54.

Amorosi, A., Centineo, M.C., 1997. Glaucony from the Eocene of the Isle of Wight (southern UK): implications for basin analysis and sequence–stratigraphic interpretation. *Journal of the Geological Society of London* 154, 887–896.

Amorosi, A., Centineo, M.C., D'Atri, A., 1997. Lower Miocene glaucony-bearing deposits in the SE Tertiary piedmont basin (northern Italy). *Rivista Italiana di Paleontologia e Stratigrafia* 103, 101–110.

Amorosi, A., Guidi, R., Mas, R., Falanga, E., 2012. Glaucony from the Cretaceous of the Sierra de Guadarrama (Central Spain) and its application in a sequence–stratigraphic context. *International Journal of Earth Sciences* 1, 415–427.

Amorosi, A., Sammartino, I., Tateo, F., 2007. Evolution patterns of glaucony maturity: a mineralogical and geochemical approach. *Deep-Sea Research Part II: Topical Studies in Oceanography* 54, 1364–1374.

Amouric, M., Parron, C., 1985. Structure and growth mechanism of glauconite as seen by high resolution transmission electron microscopy. *Clays and Clay Minerals* 33, 473–482.

Anan, T.I., 2014. Facies analysis and sequence stratigraphy of the Cenomanian–Turonian mixed siliciclastic–carbonate sediments in West Sinai, Egypt. *Sedimentary Geology* 307, 34–46.

Anderson, R.P., Fairchild, I.J., Toscac, N.J., Knoll, A.H., 2013. Microstructures in metasedimentary rocks from the Neoproterozoic Bonahaven Formation, Scotland: microconcretions, impact spherules, or microfossils? *Precambrian Research* 233, 59–72.

Arning, E.T., Lückge, A., Breuer, C., Gussone, N., Birgel, D., Peckmann, J., 2009. Genesis of phosphorite crusts off Peru. *Marine Geology* 262, 68–81.

Asensio, J.N.P., Aguirre, J., Schmiedl, G., Civis, J., 2012. Messinian paleoenvironmental evolution in the Lower Guadalquivir Basin (SW Spain) based on benthic foraminifera. *Palaeogeography Palaeoclimatology Palaeoecology* 326–328, 135–151.

Ashuri, M., Sharafi, M., Mahboubi, A., Mousavi Harami, R., Nadjafi, M., 2010. Study of genesis and mechanism of glauconite formation in the Aitamir Formation at southeast of Dargaz. *Iranian Journal of Crystallography and Mineralogy* 18, 247–254.

Bailey, S.W., 1980. Summary of recommendations of AIPEA nomenclature committee on clay minerals. *American Mineralogists* 65, 1–7.

Baioumy, H.M., 2007. Iron–phosphorus relationship in the iron and phosphorite ores of Egypt. *Chemie der Erde* 67, 229–239.

Baioumy, H.M., Boulis, S.N., 2012a. Glauconites from the Bahariya Oasis: an evidence for Cenomanian marine transgression in Egypt. *Journal of African Earth Sciences* 70, 1–7.

Baioumy, H.M., Boulis, S.N., 2012b. Non-pelletal glauconites from the Campanian Quessir Formation, Egypt: implication for glauconitization. *Sedimentary Geology* 249–250, 1–9.

Bajda, T., Kłapyta, Z., 2013. Adsorption of chromate from aqueous solutions by HDTMA-modified clinoptilolite, glauconite and montmorillonite. *Applied Clay Science* 86, 169–173.

Baker, J.C., Uwins, P.J.R., Joe Hamilton, P., 1997. Freshwater sensitivity of glauconitic hydrocarbon reservoirs. *Journal of Petroleum Science and Engineering* 18, 83–91.

Baldermann, A., Grathoff, G.H., Nickel, C., 2012. Micromilieu-controlled glauconitization in fecal pellets at Oker (Central Germany). *Clay Minerals* 47, 513–538.

Baldermann, A., Warr, L.N., Grathoff, G.H., Dietzel, M., 2013. The rate and mechanism of deep-sea glauconite formation at the Ivory Coat–Ghana marginal ridge. *Clays and Clay Minerals* 61, 258–276.

Ball, J.R., 1941. Silurian lithology in western Tennessee and adjacent States. *Geological Society of America Bulletin* 52, 1117–1128.

Bandopadhyay, P.C., 2007. Interpretation of authigenic *vs.* allogenic green peloids of ferric clay in the Proterozoic Penganga Group, southern India. *Clay Minerals* 42, 471–485.

Bandy, O.L., 1972. Neogene planktonic foraminiferal zones, California, and some geologic implications. *Palaeogeography Palaeoclimatology Palaeoecology* 12, 131–150.

Banerjee, S., Bansal, U., Pande, K., Meena, S.S., 2016. Compositional variability of glauconites within the Upper

Cretaceous Karai Shale Formation, Cauvery Basin, India: implications for evaluation of stratigraphic condensation. *Sedimentary Geology* 331, 12–29.
Banerjee, S., Chattoraj, S.L., Saraswati, P.K., Dasgupta, S., Sarkar, U., 2012b. Substrate control on formation and maturation of glauconites in the Middle Eocene Harudi Formation, western Kutch, India. *Marine and Petroleum Geology* 30, 144–160.
Banerjee, S., Chattoraj, S.L., Saraswati, P.K., Dasgupta, S., Sarkar, U., Bumby, A., 2012a. The origin and maturation of lagoonal glauconites: a case study from the Oligocene Maniyara Fort Formation, western Kutch, India. *Geological Journal* 47, 357–371.
Banerjee, S., Jeevankumar, S., Eriksson, P.G., 2008. Mg-rich ferric illite in marine transgressive and highstand systems tracts: examples from the Paleoproterozoic Semri Group, central India. *Precambrian Research* 162, 212–226.
Banerjee, S., Mondal, S., Chakraborty, P.P., Meena, S.S., 2015. Distinctive compositional characteristics and evolutionary trend of Precambrian glaucony: example from Bhalukona Formation, Chhattisgarh basin, India. *Precambrian Research* 271, 33–48.
Banning, A., Rüde, T.R., Dölling, B., 2013. Crossing redox boundaries — aquifer redox history and effects on iron mineralogy and arsenic availability. *Journal of Hazardous Materials* 262, 905–914.
Bansal, U., Banerjee, S., 2014. Influence of depositional environment on geochemical characteristics of glauconites: study from Karai Shale (Cauvery Basin) and Lameta Formation (Narmada Basin). In: *Abstract Volume, 31st Convention of Indian Association of Sedimentologists, November 12–14.* University of Pune, pp. 138–139.
Bansal, U., Banerjee, S., Pande, K., 2014. Geochemical characteristics of glauconite within transgressive deposits of Early to Late Cretaceous Karai Shale, Cauvery Basin, India. In: *Abstract Volume 19th International Sedimentological Congress, August 18–22, Geneva*, p. 45.
Baqri, S.R.H., Husain, V., Bilqees, R., Jan, N., Ahmad, N., 1994. Petrographic and chemical characteristics of glauconitic and phosphatic sediments of the Kussak Formation, Khewra Gorge, Salt Range, Pakistan. *Pakistan Journal of Scientific and Industrial Research* 37, 291–296.
Barringer, J.L., Mumford, A., Young, L.Y., Reilly, P.A., Bonin, J.L., Rosman, R., 2010. Pathways for arsenic from sediments to groundwater to streams: biogeochemical processes in the Inner Coastal Plain, New Jersey, USA. *Water Research* 44, 5532–5544.
Barusseau, J.P., Giresse, P., Faure, H., Lezine, A.M., Masse, J.P., 1988. Marine sedimentary environments on some parts of the tropical and equatorial Atlantic margins of Africa during the Late Quaternary. *Continental Shelf Research* 8, 1–21.
Basa, T., Greensmith, J.T., Finzi, C.V., 1997. The sub-surface Holocene Middle sands of Dungeness. *Proceedings of the Geologists' Association* 108, 105–112.
Basu, A., Bickford, M.E., 2014. Contributions of zircon U–Pb geochronology to understanding the volcanic and sedimentary history of some Purana basins, India. *Journal of Asian Earth Sciences* 91, 252–262.
Bau, M., Alexander, B., Chesley, J.T., Dulski, P., Brantley, S.L., 2004. Mineral dissolution in the Cape Cod aquifer, Massachusetts, USA: I. Reaction stoichiometry and impact of accessory feldspar and glauconite on strontium isotopes, solute concentrations, and REY distribution. *Geochimica et Cosmochimica Acta* 68, 1199–1216.
Bell, D.L., Goodell, G., 1967. A comparative study of glauconite and the associated clay fraction in modern marine sediments. *Sedimentology* 9, 169–202.
Bentor, K., Kastner, M., 1965. Notes on the mineralogy and origin of glauconite. *Journal of Sedimentary Petrology* 35, 155–166.
Berg-Madsen, V., 1983. High-alumina glaucony from the Middle Cambrian of Orland and Bornholm, southern Baltoscandia. *Journal of Sedimentary Petrology* 53, 875–893.
Berra, F., Zanchi, A., Mattei, M., Nawab, A., 2007. Late Cretaceous transgression on a Cimmerian high (Neka Valley, Eastern Alborz, Iran): a geodynamic event recorded by glauconitic sands. *Sedimentary Geology* 199, 189–204.
Bhattacharyya, A., Chanda, S.K., Friedman, G.M., 1986. Dolomitized glauconite granules: a new kind of peloid from Proterozoic strata of Central India. *Journal of Sedimentary Petrology* 56, 480–485.
Birch, G.F., 1979. The nature and origin of mixed apatite/glauconite pellets from the continental shelf off South Africa. *Marine Geology* 29, 313–334.
Bitschene, P.R., Holmes, M.A., Breza, J.R., 1992. Composition and origin of Cr-rich glauconitic sediments from the southern Kerguelen Plateus (Site 748). *Proceedings of the Ocean Drilling Program, Scientific Results* 120, 113–134.
Bjerkli, K., Östmo-Saeter, J.S., 1973. Formation of glauconite in foraminiferal shells on the continental shelf off Norway. *Marine Geology* 14, 169–178.
Böhm, F., 1986. The grimming: upper Triassic to Middle Jurassic history of a Carbonate platform (Northern Alps, Austria). *Facies* 15, 195–231.
Bornhold, B.D., Giresse, P., 1985. Glauconitic sediments on the continental shelf off Vancouver Island, British Columbia, Canada. *Journal of Sedimentary Petrology* 55, 653–664.
Boukhalfa, K., Amorosi, A., Soussi, M., Ismail-Lattrâche, K.B., 2015. Glauconitic-rich strata from Oligo-Miocene shallow-marine siliciclastic deposits of the northern margin of Africa (Tunisia): geochemical approach for basin analysis. *Arabian Journal of Geosciences* 8, 1731–1742.
Boyer, P.S., Guinness, E.A., Blosse, M.A.L., Stolzman, R.A., 1977. Greensand fecal pellets from New Jersey. *Journal of Sedimentary Petrology* 47, 267–280.
Bozkaya, Ö., Yalçin, H., 2013. Geochemical monitoring of clays for diagenetic evolution of the Paleozoic–Lower Mesozoic sequence in the northern Arabian plate: Hazro and Amanos regions, Southeastern Turkey. *Journal of African Earth Sciences* 86, 10–24.
Brandano, M., Civitelli, G., 2007. Non-seagrass meadow sedimentary facies of the Pontinian Islands, Tyrrhenian Sea: a modern example of mixed carbonate–siliciclastic sedimentation. *Sedimentary Geology* 201, 286–301.
Brasier, M.D., 1980. The Lower Cambrian transgression and glauconite-phosphatic facies in Western Europe. *Journal of the Geological Society London* 137, 695–703.
Breheret, J.G., 1991. Glauconitization episodes in marginal settings as echoes of Mid-Cretaceous anoxic events recorded in the Vocontian Basin. *Geological Society, London, Special Publications* 58, 415–425.
Buatier, M., Honnorez, J., Ehret, G., 1989. Fe-smectite–glauconite transition in hydrothermal green clays from the Galapagos spreading center. *Clays and Clay Minerals* 37, 532–541.
Burnett, W.C., 1980. Apatite-glauconite associations off Peru and Chile: Palaeo-oceanographic implications. *Journal of Geological Society London* 137, 757–764.
Burst, J.F., 1958a. 'Glauconite' pellets: their mineral nature and applications to stratigraphic interpretations. *American Association of Petroleum Geologists Bulletin* 42, 310–327.
Burst, J.F., 1958b. Mineral heterogeneity in glauconite pellets. *American Mineralogists* 43, 481–497.
Cairncross, B., Hart, R.J., Willis, J.P., 1990. Geochemistry and sedimentology of coal seams from the Permian Witbank Coalfield, South Africa, a means of identification. *International Journal of Coal Geology* 16, 309–325.
Cao, J., Zhang, Y.S., Song, T.R., Wang, J.T., 2010. Mineralogical evidences and significance of transgression event in the

Cretaceous basins of eastern Heilongjiang Province, China. *Geological Bulletin of China* 29, 1024–1030 (in Chinese with English abstract).
Caracciolo, L., Le Pera, E., Muto, F., Perri, F., 2011. Sandstone petrology and mudstone geochemistry of the Peruc–Korycany Formation (Bohemian Cretaceous Basin, Czech Republic). *International Geology Review* 53, 1003–1031.
Carson, G.A., Crowley, S.F., 1993. The glauconite-phosphate association in hardgrounds: examples from the Cenomanian of Devon, southwest England. *Cretaceous Research* 14, 69–89.
Carter, L., 1975. Sedimentation on the continental terrace around New Zealand: a review. *Marine Geology* 19, 209–237.
Cas, R.A.S., Landis, C.A., Fordyce, R.E., 1989. A monogenetic, Surtla-type, Surtseyan volcano from the Eocene–Oligocene Waiareka–Deborah volcanics, Otago, New Zealand: a model. *Bulletin of Volcanology* 51, 281–298.
Cecil, M.R., Ducea, M.N., 2011. K–Ca ages of authigenic sediments: examples from Paleozoic glauconite and applications to low-temperature thermochronometry. *International Journal of Earth Sciences* 100 (8), 1783–1790.
Chafetz, H.S., 1978. A trough cross-stratified glaucarenite: a Cambrian tidal inlet accumulation. *Sedimentology* 25, 545–559.
Chafetz, H.S., 2007. Paragenesis of the Morgan Creek Limestone, Late Cambrian, Central Texas: constraints on the formation of glauconite. *Deep-Sea Research II* 54, 1350–1363.
Chafetz, H.S., Reid, A., 2000. Syndepositional shallow water precipitation of glauconitic minerals. *Sedimentary Geology* 136, 29–42.
Chang, S.S., Shau, Y.H., Wang, M.K., Ku, C.T., Chiang, P.N., 2008. Mineralogy and occurrence of glauconite in central Taiwan. *Applied Clay Science* 42, 74–80.
Charpentier, D., Buatier, M.D., Jacquot, E., Gaudin, A., Wheat, C.G., 2011. Conditions and mechanism for the formation of iron-rich montmorillonite in deep-sea sediments (Costa Rica margin); coupling high-resolution mineralogical characterization and geochemical modelling. *Geochimica et Cosmochimica Acta* 75, 1397–1410.
Chattoraj, S.L., Banerjee, S., Saraswati, P.K., 2009. Glauconites from the Late Palaeocene–Early Eocene Naredi Formation, western Kutch and their genetic implications. *Journal of Geological Society of India* 73, 567–574.
Chen, H.Z., Chen, S.P., 1997. Mineralogical and distributive characteristics of glauconite in sediment in Taiwan Strait. *Journal of Oceanography in Taiwan Strait* 16 (3), 355–362.
Chen, L.R., Duan, W.M., 1987. Formation of glauconite as infillings of organism. *Acta Sedimentologica Sinica* 5 (3), 171–179 (in Chinese with English abstract).
Chen, L.R., Yu, X., Shi, Y.M., 1980. Glauconite in the sediments of East China Sea. *Chinese Journal of Geology* 15 (3), 205–217 (in Chinese with English abstract).
Chen, R.J., 1980. Characteristics of glauconites from some regions and their significance in analyzing the facies environment. *Chinese Journal of Geology* 15 (1), 65–75 (in Chinese with English abstract).
Chen, R.J., 1983. Study of glauconites from Beibu bay of the South China Sea. *Chinese Journal of Geology* 18 (3), 267–272 (in Chinese with English abstract).
Chen, R.J., Fan, D.L., Wang, D.G., Wang, Z.C., 1988. Mineralogical study of glauconite in a Cambrian–Ordovician profile at Xiaoyangqiao area, Dayangcha, Jilin Province. *Chinese Journal of Geology* 23 (1), 68–80 (in Chinese with English abstract).
Cimbálníková, A., 1971. Chemical variability and structural heterogeneity of glauconites. *American Mineralogist* 56, 1385–1398.
Clark, M., Robertson, A., 2005. Uppermost Cretaceous–Lower Tertiary Ulukişla Basin, South–Central Turkey: sedimentary evolution of part of a unified basin complex within an evolving Neotethyan suture zone. *Sedimentary Geology* 173, 15–51.
Compton, J.S., Wiltshire, J.G., 2009. Terrigenous sediment export from the western margin of South Africa on glacial/interglacial cycles. *Marine Geology* 266, 212–222.
Conrad, J., Hein, J., Chaudhuri, A., Deb, S.P., Mukhopadhyay, J., Deb, G.K., Beukes, N.J., 2011. Constraints on the development of Proterozoic basins in Central India from $^{40}Ar/^{39}Ar$ analysis of authigenic glauconitic minerals. *Geological Society of America Bulletin* 123, 158–167.
Cook, P.J., Marshall, J.F., 1981. Geochemistry of iron and phosphorus-rich nodules from the East Australian continental shelf. *Marine Geology* 41, 205–221.
Ćosović, V., Drobne, K., 1995. Palaeoecological significance of morphology of orthophragminids from the Istrian Peninsula (Croatia and Slovenia). *Geobios* 18, 93–99.
Ćosović, V., Drobne, K., Moro, A., 2004. Palaeoenvironmental model for Eocene foraminiferal limestones of the Adriatic carbonate platform (Istrian Peninsula). *Facies* 50, 61–75.
Courbe, C., Velde, B., Meunier, A., 1981. Weathering of glauconites: reversal of the glauconitization process in a soil profile in western France. *Clay Minerals* 16, 231–243.
Cuadros, J., Dekov, V.M., Arroyo, X., Nieto, F., 2011. Smectite formation in submarine hydrothermal sediments: samples from the HMS Challenger Expedition (1872–1776). *Clays and Clay Minerals* 59, 147–164.
Czuryłowicz, K., Lejzerowicz, A., Kowalczyk, S., Wysocka, A., 2014. The origin and depositional architecture of Paleogene quartz-glauconite sands in the Lubartów area, eastern Poland. *Geological Quarterly* 58, 125–144.
Das, P.K., Duarah, B.P., 1993. Glauconites in some carbonate rocks of Garo Hills. *Bulletin of Pure and Applied Sciences, Section F: Geological Sciences* 12F, 25–30.
Dasgupta, S., Chaudhuri, A.K., Fukuoka, M., 1990. Compositional characteristics of glauconitic alterations of K-feldspar from India and their implications. *Journal of Sedimentary Petrology* 60, 277–281.
Day, E.S., James, N.P., Narbonne, G.M., Dalrymple, R.W., 2004. A sedimentary prelude to Marinoan glaciation, Cryogenian (Middle Neoproterozoic) Keele Formation, Mackenzie Mountains, northwestern Canada. *Precambrian Research* 133, 223–247.
De Ros, L.F., Morad, S., A1-Aasm, I.S., 1997. Diagenesis of siliciclastic and volcaniclastic sediments in the Cretaceous and Miocene sequences of the NW African margin (DSDP Leg 47A, Site 397). *Sedimentary Geology* 112, 137–156.
Deb, S.P., Fukuoka, M., 1998. Fe-illites in a Proterozoic deep marine slope deposit in the Penganga Group of the Pranhita Godavari Valley: their origin and environmental significance. *The Journal of Geology* 106, 741–750.
Debrabant, P., Paquet, J., 1975. L'association glauconites-phosphates-carbonates (Albien de la Sierra de Espuna, Espagne meridionale). *Chemical Geology* 15, 61–75.
Deconinck, J.F., Strasser, A., 1987. Sedimentology, clay mineralogy and depositional environment of Purbeckian green marls (Swiss and French Jura). *Eclogae Geologicae Helvetiae* 80, 753–772.
Delamette, M., 1989. Trace fossil assemblages from the Albian phosphate-rich sandstones of the Helvetic Shelf (Western Alps). *Cretaceous Research* 10, 207–219.
Demirpolat, S., 1991. Surface and near-surface sediments from the continental shelf off the Russian River, northern California. *Marine Geology* 99, 163–173.
Dias, J.M.A., Nittrouer, C.A., 1984. Continental shelf sediments of northern Portugal. *Continental Shelf Research* 3, 147–165.
Díez-Canseco, D., Arz, J.A., Benito, M., Díaz-Molina, M., Arenillas, I., 2014. Tidal influence in redbeds: a palaeoenvironmental and biochronostratigraphic

reconstruction of the Lower Tremp Formation (South–Central Pyrenees, Spain) around the Cretaceous/Paleogene boundary. *Sedimentary Geology* 312, 31–49.

Dill, C.E., 1969. The formation and distribution of glauconite on the North Carolina continental shelf and slope. *Abstract in: Geological Society of America Special Paper* 121, 431–432.

Dill, H.G., Scheel, M., Köthe, A., Botz, R., Henjes-Kunst, F., 1996. An integrated environment analysis lithofacies, chemofacies, biofacies of the Oligocene calcareous–siliciclastic shelf deposits in northern Germany. *Palaeogeography Palaeoclimatology Palaeoecology* 31, 145–174.

Dix, G.R., Parras, A., 2014. Integrated diagenetic and sequence stratigraphy of a Late Oligocene–Early Miocene, mixed-sediment platform (Austral Basin, southern Patagonia): resolving base-level and paleoceanographic changes, and paleoaquifer characteristics. *Sedimentary Geology* 307, 17–33.

Drits, V.A., Ivanovskaya, T.A., Sakharov, B.A., Zvyagina, B.B., Derkowski, A., Gor̀kova, N.V., Pokrovskaya, E.V., Savichev, A.T., Zaitseva, T.S., 2010. Nature of the structural and crystal-chemical heterogeneity of the Mg-rich glauconite (Riphean, Anabar Uplift). *Lithology and Mineral Resources* 45, 555–576.

Duarte, M.A., Martínez, M.L., 2002. K–Ar dating and geological significance of clastic sediments of the Paleocene Sepultura Formation, Baja California, México. *Journal of South American Earth Sciences* 15, 725–730.

Duplay, J., Buatier, M., 1990. The problem of differentiation of glauconite and celadonite. *Chemical Geology* 84, 264–266.

Dustira, A.M., Wignall, P.B., Joachimski, M., Blomeier, D., Fröder, C.H., Bond, D.P.G., 2013. Gradual onset of anoxia across the Permian–Triassic Boundary in Svalbard, Norway. *Palaeogeography Palaeoclimatology Palaeoecology* 374, 303–313.

Dypvik, H., Nagy, J., Krinsley, D.H., 1992. Origin of the Myklegardfjellet Bed, a basal Cretaceous marker on Spitsbergen. *Polar Research* 11 (1), 21–31.

Eder, V.G., Martín-Algarra, A., Sánchez-Navas, A., Zanin, Y.N., Zamirailova, A.G., Lebedev, Y.N., 2007. Depositional controls on glaucony texture and composition, Upper Jurassic, West Siberian Basin. *Sedimentology* 54, 1365–1387.

Egenhoff, S., 2004. The Ordovician succession on Baltica — carbonate ramp or epicontinental sea?. In: *The 26th Nordic Winter Meeting, Uppsala, Abstract Volume: GFF*, vol. 126, pp. 160–161.

Ehlmann, A., Hulings, N., Glover, E., 1963. Stages of glauconite formation in modern foraminiferal sediments. *Journal of Sedimentary Petrology* 33, 87–96.

Eickmann, B., Bach, W., Kiel, S., Reitner, J., Peckmann, J., 2009. Evidence for cryptoendolithic life in Devonian pillow basalts of Variscan orogens, Germany. *Palaeogeography Palaeoclimatology Palaeoecology* 283, 120–125.

El Albani, A., Fürsich, F.T., Colin, J.P., Meunier, A., Hochuli, P., Closas, C.M., Mazin, J.-M., Billon-Bruyat, J.-P., 2004. Palaeoenvironmental reconstruction of the basal Cretaceous vertebrate bearing beds in the northern part of the Aquitaine Basin (SW France): sedimentological and geochemical evidence. *Facies* 50, 195–215.

El Albani, A., Meunier, A., Fürsich, F., 2005. Unusual occurrence of glauconite in a shallow lagoonal environment (Lower Cretaceous, northern Aquitaine Basin, SW France). *Terra Nova* 17, 537–544.

El Kadiri, K., Serrano, F., Hlila, R., Liemlahi, H., Chalouan, A., Lopez-Garrido, A.C., Guerra-Merch, A., Sanz-de-Galdeano, C., Kerzazi, K., El Mrihi, A., 2005. Lithostratigraphy and sedimentology of the latest Cretaceous–early Burdigalian Tamezzakht succession (Northern Rif, Morocco): consequences for its sequence stratigraphic interpretation. *Facies* 50, 477–503.

El-Azabi, M.H., El-Araby, A., 2007. Depositional framework and sequence stratigraphic aspects of the Coniacian–Santonian mixed siliciclastic/carbonate Matulla sediments in Nezzazat and Ekma blocks, Gulf of Suez, Egypt. *Journal of African Earth Sciences* 47, 179–202.

El-Ghali, M.A.K., Morada, S., Mansurbega, H., Cajae, M.A., Sirat, M., Ogle, N., 2009. Diagenetic alterations related to marine transgression and regression fluvial and shallow marine sandstones of the Triassic Buntsandstein and Keuper sequence, the Paris Basin, France. *Marine and Petroleum Geology* 26, 289–309.

Engalychev, S.Y., Panova, E.G., 2011. Geochemistry and genesis of sandstones of eastern part of Main Devonian field in the northwestern part of the Russian Plate. *Lito-sfera* 5, 16–29.

Eoff, J., 2014. Sequence stratigraphy of the Upper Cambrian (Furongian; Jiangshanian and Sunwaptan) Tunnel City Group, Upper Mississippi Valley: transgressing assumptions of cratonic flooding. *Sedimentary Geology* 302, 87–101.

Erba, E., 1994. Nannofossils and superplumes: the early Aptian "nannoconid crisis". *Paleoceanography* 9, 483–501.

Erbacher, J., Thurow, J., Littke, R., 1996. Evolution patterns of radiolaria and organic matter variations: a new approach to identify sea level changes in Mid-Cretaceous pelagic environments. *Geology* 24, 499–502.

Eriksson, M.E., Lindskog, A., Calner, M., Mellgren, J.I.S., Bergström, S.M., Terfelt, F., Schmitz, B., 2012. Biotic dynamics and carbonate microfacies of the conspicuous Darriwilian (Middle Ordovician) 'Täljsten' interval, South–Central Sweden. *Palaeogeography, Palaeoclimatology, Palaeoecology* 367–368, 89–103.

Ershova, V.B., 2008. Glauconite from Latorpian Regional Stage (Lower Ordovician) from Leningrad district. *Vestnik Sankt-Peterburgskogo Universiteta, Seriya Geologiya i Geografiya* 1, 15–19.

Fanning, D.S., Rabenhorst, M.C., Balduff, D.M., Wagner, D.P., Orr, R.S., Zurheide, P.K., 2010. An acid sulfate perspective on landscape/seascape soil mineralogy in the U.S. Mid-Atlantic region. *Geoderma* 154, 457–464.

Farouk, S., 2015. Upper Cretaceous sequence stratigraphy of the Galala Plateaux, western side of the Gulf of Suez, Egypt. *Marine and Petroleum Geology* 60, 136–158.

Ferrow, E., Vajda, V., Koch, C.B., Peucker-Ehrenbrink, B., Willumsen, P.S., 2011. Multiproxy analysis of a new terrestrial and a marine Cretaceous–Paleogene (K–Pg) boundary site from New Zealand. *Geochimica et Cosmochimica Acta* 75, 657–672.

Fiet, N., Quidelleur, X., Pariz, O., Bulot, L.G., Gillot, P.Y., 2006. Lower Cretaceous stage durations combining radiometric data and orbital chronology: towards a more stable relative time scale? *Earth and Planetary Science Letters* 246, 407–417.

Fischer, H., 1987. Excess K–Ar ages of glauconite from the Upper Marine Molasse and evidence for glauconitization of mica. *Geologische Rundschau* 76 (3), 885–902.

Fitch, F.J., Hooker, P.J., Miller, J.A., Brereton, N.R., 1978. Glauconite dating of Palaeocene–Eocene rocks from East Kent and the time-scale of Palaeogene volcanism in the North Atlantic region. *Journal of the Geological Society* 135, 499–512.

Foland, K.A., Linder, J.S., Laskowski, T.E., Grant, N.K., 1984. $^{40}Ar/^{39}Ar$ dating of glauconites: measured ^{39}Ar recoil loss from well-crystallized specimens. *Chemical Geology* 2, 241–264.

Föllmi, K.B., Breymann, M.V., 1992. Phosphates and glauconites of Sites 798 and 799. *Proceedings of the Ocean Drilling Program, Scientific Results* 127–128, 63–74.

Franzosi, C., Castro, L.N., Celeda, A.M., 2014. Technical evaluation of glauconites as alternative potassium fertilizer from the Salamanca Formation, Patagonia, Southwest Argentina. *Natural Resources Research* 23, 311–320.

Friis, H., Poulsen, M.L.K., Svendsen, J.B., Hamberg, L., 2007. Discrimination of density flow deposits using elemental geochemistry — implications for subtle provenance differentiation in a narrow submarine canyon, Paleogene, Danish North Sea. *Marine and Petroleum Geology* 24, 221–235.

Furquim, S.A.C., Barbiéro, L., Graham, R.C., Neto, J.P.Q., Ferreira, R.P.D., Furian, S., 2010. Neoformation of micas in soils surrounding an alkaline-saline lake of Pantanal wetland, Brazil. *Geoderma* 158, 331–342.

Fürsich, F.T., 1984. Palaeoecology of Boreal invertebrate faunas from the Upper Jurassic of central East Greenland. *Palaeogeography, Palaeoclimatology, Palaeoecology* 48, 309–364.

García-García, F., De Gea, G.A., Ruiz-Ortiz, P.A., 2011. Detached forced-regressive shoreface wedges at the southern Iberian continental palaeomargin (Early Cretaceous, Betic Cordillera, S Spain). *Sedimentary Geology* 236, 197–210.

Garrison, R.E., Kennedy, W.J., Palmer, T.J., 1987. Early lithification and hardgrounds in Upper Albian and Cenomanian Calcarenites, Southwest England. *Cretaceous Research* 8, 103–140.

Garzanti, E., Angiolini, L., Brunton, H., Sciunnach, D., Balini, M., 1998. The Bashkirian "Fenestella Shales" and the Moscovian "Chaetetid Shales" of the Tethys Himalaya (South Tibet, Nepal and India). *Journal of Asian Earth Sciences* 16, 119–141.

Garzanti, E., Haas, R., Jadoul, F., 1989. Ironstones in the Mesozoic passive margin sequence of the Tethys Himalaya (Zanskar, Northern India): sedimentology and metamorphism. In: Young, T.P., Taylor, W.E.G. (Eds.), *Phanerozoic Ironstones, Geological Society Special Publication*, 46, pp. 229–244.

Gaudin, A., Buatier, M.D., Beaufort, D., Petit, S., Grauby, O., Decarreau, A., 2005. Characterization and origin of Fe^{3+}-montmorillonite in deep-water calcareous sediments (Pacific Ocean, Costa Rica Margin). *Clays and Clay Minerals* 53, 452–465.

Ge, R.Q., 2004. Occurrence and geological significance of glauconite in Cenozoic Group of Jiyang depression. *Acta Sedimentologica Sinica* 22, 276–280 (in Chinese with English abstract).

Gebhart, G., 1982. Glauconitic condensation through high-energy events in the Albian near Clars (Escragnolles, Vat, SE France). In: Einsele, G., Seilacher, A. (Eds.), *Cyclic and Event Stratification.* Springer Verlag, Berlin, pp. 286–298.

Geptner, A.R., Ivanovskaya, T.A., Pokrovskaya, E.V., Kuralenko, N.P., 2008. Glauconite from Paleogene volcano-terrigenous rocks in western Kamchatka. *Lithology and Mineral Resources* 43 (3), 228–249.

Ghabeishavi, A., Moghaddam, H.V., Taheri, A., 2009. Facies distribution and sequence stratigraphy of the Coniacian–Santonian succession of the Bangestan Palaeo-high in the Bangestan Anticline, SW Iran. *Facies* 55, 243–257.

Gier, S., Worden, R.H., Johns, W.D., Kurzweil, H., 2008. Diagenesis and reservoir quality of Miocene sandstones in the Vienna Basin, Austria. *Marine and Petroleum Geology* 25, 681–695.

Giresse, P., Bassetti, M.A., Chanier, F., Gaullier, V., Maillard, A., Thinon, I., Lofi, J., Lymer, G., Reynaud, J.-Y., Negri, A., Saavedra-Pellitero, M., 2015. Depositional environment and age of some key Late Pliocene to Early Quaternary deposits on the underfilled Cedrino paleovalley (Orosei): insight into the Neogene geodynamic evolution of Sardinia. *Quaternary International* 357, 220–236.

Giresse, P., Wiewióra, A., 2001. Stratigraphic condensed deposition and diagenetic evolution of green clay minerals in deep water sediments on the Ivory Coast–Ghana Ridge. *Marine Geology* 179, 51–70.

Giresse, P., Wiewióra, A., Grabska, D., 2004. Glauconitization processes in the northwestern Mediterranean (Gulf of Lions). *Clay Minerals* 39, 57–73.

Giresse, P., Wiewióra, A., Lacka, B., 1988. Mineral phases and processes within green peloids from two recent deposits near the Congo River Mouth. *Clay Minerals* 23, 447–458.

Glenn, C.R., Arthur, M.A., 1990. Anatomy and origin of a Cretaceous phosphorite-greensand giant, Egypt. *Sedimentology* 37, 123–154.

Godek, G., Beauchamp, B., 2011. Iron from land: the origin of Middle Permian (Trold Fiord) glauconite in the Sverdrup Basin, Arctic Canada. Recovery — 2011 CSPG CSEG CWLS Convention.

Godet, A., Föllmi, K.B., Bodin, S., de Kaenel, E., Matera, V., Adatte, T., 2010. Stratigraphic sedimentological and palaeoenvironmental constraints on the rise of the Urgonian platform in the western Swiss Jura. *Sedimentology* 57, 1088–1125.

Godet, A., Föllmi, K.B., Stille, P., Bodin, S., Matera, V., Adatte, T., 2011. Reconciling strontium-isotope and K–Ar ages with biostratigraphy: the case of the Urgonian platform, Early Cretaceous of the Jura Mountains, Western Switzerland. *Swiss Journal of Geosciences* 104, 147–160.

Gomez, F.J., Astini, R.A., 2015. Sedimentology and sequence stratigraphy from a mixed (carbonate–siliciclastic) rift to passive margin transition: the Early to Middle Cambrian of the Argentine Precordillera. *Sedimentary Geology* 316, 39–61.

Grant, N.K., Laskowski, T.E., Foland, K.A., 1984. Rb–Sr and K–Ar ages of Paleozoic glauconites from Ohio-Indiana and Missouri, USA. *Chemical Geology* 65, 303.

Griffioen, J., Klein, J., Van Gaans, P.F., 2012. Reaction capacity characterization of shallow sedimentary deposits in geologically different regions of the Netherlands. *Journal of Contaminant Hydrology* 127, 30–46.

Guimaraes, E.M., Velde, B., Hillier, S., 2000. Diagenetic/anchimetamorphic changes on the Proterozoic glauconite and glaucony from the Paranoa grour mid-western Brazil. *Brazilian Journal of Geology* 30 (3), 363–366.

Gulbrandsen, R.A., Goldich, S.S., Thomas, H.H., 1963. Glauconite from the Precambrian Belt Series, Montana. *Science* 140, 390–391.

Guo, X.P., 1991. An approach to the depositional environment of the cretaceous Kizilsu Group: the lowermost marine horizon of the Cretaceous in the western Tarim Basin. *Acta Geological Sinica* 65 (2), 188–198 (in Chinese with English abstract).

Gygi, R.A., Marchand, D., 1982. Les faunes de *Cardioceratinae (Ammonoidea)* du Callovien terminal et de l'Oxfordien inférieur et moyen (Jurassique) de la Suisse septentrionale: Stratigraphie, paléoécologie, taxonomie préliminaire. *Geobios* 15 (4), 517–571.

Hallam, A., Maynard, J.B., 1987. The iron ores and associated sediments of the Chichali formation (Oxfordian to Valanginian) of the Trans-Indus Salt Range, Pakistan. *Journal of the Geological Society, London* 144, 107–114.

Harding, S.C., 2014. *Ichnology, Mineralogy, and Paleoenvironmental Implications of the Verdine and Glaucony Facies in Sedimentary Rocks* (Ph.D., Dissertation). University of Utah, p. 237.

Harris, L.C., Whiting, B.M., 2000. Sequence-stratigraphic significance of Miocene to Pliocene glauconite-rich layers, on- and offshore of the US Mid-Atlantic Margin. *Sedimentary Geology* 134, 129–147.

Harris, W.B., 1976. Rb–Sr glauconite isochron, Maestrichtian unit of Peedee Formation (Upper Cretaceous), North Carolina. *Geology* 4, 761–762.

Harris, W.B., Bottino, M.L., 1974. Rb–Sr study of Cretaceous Lobate Glauconite Pellets, North Carolina. *Geological Society of America Bulletin* 85, 1475–1478.

Hart, M.B., 1999. The evolution and biodiversity of Cretaceous planktonic foraminifera. *Geobios* 32, 247–255.

Henderson, R.A., 1998. Eustatic and palaeoenvironmental assessment of the Mid-Cretaceous Bathurst Island Group of the Money Shoals Platform, northern Australia. *Palaeogeography, Palaeoclimatology, Palaeoecology* 138, 115–138.

Hesse, R., Von Rad, U., Fabricius, F.H., 1971. Holocene sedimentation in the Strait of Otranto between the Adriatic and Ionian Seas (Mediterranean). *Marine Geology* 10, 293–355.

Hesselbo, S.P., Huggett, J.M., 2001. Glaucony in ocean-margin sequence stratigraphy (Oligocene–Pliocene, Offshore New Jersey, USA; ODP Leg 174A). *Journal of Sedimentary Research* 71, 598–606.

Howe, J.A., Pudsey, C.J., Cunningham, A.P., 1997. Pliocene–Holocene contourite deposition under the Antarctic Circumpolar Current, western Falkland Trough, South Atlantic Ocean. *Marine Geology* 138, 27–50.

Hower, J., 1961. Some factors concerning the nature and the origin of glauconite. *American Mineralogist* 46, 313–334.

Huggett, J.M., Cuadros, J., 2010. Glauconite formation in lacustrine/palaeosol sediments, Isle of Wight (Hampshire Basin), UK. *Clay Minerals* 45, 35–49.

Huggett, J.M., Gale, A.S., 1997. Petrology and palaeoenvironmental significance of glaucony in the Eocene succession at Whitecliff Bay, Hampshire Basin, U.K. *Journal of the Geological Society of London* 154, 897–912.

Huggett, J.M., Gale, A.S., McCarty, D., 2010. Petrology and palaeoenvironmental significance of authigenic iron-rich clays, carbonates and apatite in the Claiborne Group, Middle Eocene, NE Texas. *Sedimentary Geology* 228, 119–139.

Hughes, A.D., Whitehead, D., 1987. Glauconitization of detrital silica substrates in the Barton Formation (Upper Eocene) of the Hampshire Basin, southern England. *Sedimentology* 34, 825–835.

Huisman, D.J., Vermeulen, F.J.H., Baker, J., Veldkomp, A., Krooneberg, S.B., Klaver, G.Th, 1997. A geological interpretation of heavy metal concentrations in soils and sediments in the southern Netherlands. *Journal of Geochemical Exploration* 59, 163–174.

Humez, P., Lagneau, V., Lions, J., Negrel, P., 2013. Assessing the potential consequences of CO_2 leakage to freshwater resources: a batch-reaction experiment towards an isotopic tracing tool. *Applied Geochemistry* 30, 178–190.

Humphreys, B., Balson, P.S., 1985. Authigenic glaucony in the East Anglian Crags. *Proceedings of the Geologists' Association* 96 (2), 183–188.

Ireland, B.J., Curtis, C.D., Whiteman, J.A., 1983. Compositional variation within some glauconites and illites and implications for their stability and origins. *Sedimentology* 30, 769–786.

Isaac, M.J., Moore, P.R., Joass, Y.J., 1991. Tahora Formation: the basal facies of a Late Cretaceous transgressive sequence, northeastern New Zealand. *New Zealand Journal of Geology and Geophysics* 34 (2), 227–236.

Ivanovskaya, T.A., Geptner, A.R., 2004. Glauconite at different stages of lithogenesis in Lower Cambrian rocks of western Lithuania. *Lithology and Mineral Resources* 39, 191–202.

Ivanovskaya, T.A., Geptner, A.R., Savichev, A.T., Pokrovskii, B.G., Pokrovskaya, E.V., 2014. Siderite micro-concretions in the glauconite-bearing clayey-silty rocks of the Khaipakh Formation (Middle Riphean, Olenek Uplift). *Lithology and Mineral Resources* 49, 519–545.

Ivanovskaya, T.A., Goŕkova, N.V., Karpova, G.V., Pokrovskaya, E.V., 2006. Layer silicates (glauconite, illite, and chlorite) in terrigenous rocks of the Arymash Formation (Olenek Uplift). *Lithology and Mineral Resources* 6, 601–623.

Ivanovskaya, T.A., Zaitseva, T.S., Zvyagina, B.B., Sakharov, B.A., 2012. Crystal chemical peculiarities of globular layer silicates of the glauconite–illite composition (Upper Proterozoic, northern Siberia). *Lithology and Mineral Resources* 6, 491–512.

Jamoussi, F., 1991. *Etude géologique et géotechnique des substances minérales utiles de la région de Gafsa (Sud de la Tunisie), minéralogie, géochimie et application industrielle* (Thèse de doctorat de spécialité en géologie). Faculté des sciences de Tunis, p. 298 (in French).

Jarrar, G., Amireh, B., Zachmann, D., 2000. The major, trace and rare earth element geochemistry of glauconites from the Early Cretaceous Kurnub Group of Jordan. *Geochemical Journal* 34, 207–222.

Jiang, Z., Chen, D., Qiu, L., Liang, H., Ma, J., 2007. Source-controlled carbonates in a small Eocene half-graben lake basin (Shulu Sag) in central Hebei Province, North China. *Sedimentology* 54, 265–292.

Jiménez-Millán, J., Castro, J.M., 2008. K-feldspar alteration to gel material and crystallization of glauconitic peloids with berthierine in Cretaceous marine sediments–sedimentary implications (Prebetic Zone, Betic Cordillera, SE Spain). *Geological Journal* 43, 19–31.

Jiménez-Millán, J., Molina, J.M., Nieto, F., Nieto, L., Ortiz, P.A.R., 1998. Glauconite and phosphate peloids in Mesozoic carbonate sediments (Eastern Subbetic Zone, Betic Cordilleras, SE Spain). *Clay Minerals* 33, 547–559.

John, C.M., Karner, G.D., Browning, E., Leckie, R.M., Mateo, Z., Carson, B., Lowery, C., 2011. Timing and magnitude of Miocene eustasy derived from the mixed siliciclastic–carbonate stratigraphic record of the northeastern Australian margin. *Earth and Planetary Science Letters* 304, 455–467.

Kale, V., Peshwa, V.V., 1995. *Bhima Basin*. Geological Society of India, Bangalore, p. 142.

Kalia, P., Kintso, R., 2006. Planktonic foraminifera at the Paleocene/Eocene boundary in the Jaisalmer Basin, Rajasthan, India. *Micropaleontology* 52, 521–536.

Kaya, A., Friedman, G.M., 1997. Sedimentation and significance of the nuia-bearing units in the lower Middle Ordovician antelope valley limestone (AVL) in Central Nevada, USA. *Carbonates and Evaporites* 12 (2), 276–295.

Kelly, J.C., Webb, J.A., 1999. The genesis of glaucony in the Oligo-Miocene Torquay Group, southeastern Australia: petrographic and geochemical evidence. *Sedimentary Geology* 125, 99–114.

Kelly, J.C., Webb, J.A., Maas, R., 2001. Isotopic constraints on the genesis and age of autochthonous glaucony in the Oligo-Miocene Torquay Group, south-eastern Australia. *Sedimentology* 48, 325–338.

Ketzer, J.M., Holz, M., Morad, S., Al-Aasm, I.S., 2003. Sequence stratigraphic distribution of diagenetic alterations in coal-bearing, paralic sandstones: evidence from the Rio Bonito Formation (Early Permian), southern Brazil. *Sedimentology* 50, 855–877.

Khalifa, M.A., 1983. Origin and occurrence of glauconite in the green sandstone associated with unconformity, Bahariya Oases, Western Desert, Egypt. *Journal of African Earth Sciences* 1, 321–325.

Kim, Y., Lee, Y.I., 2000. Ironstones and green marine clays in the Dongjeom Formation (Early Ordovician) of Korea. *Sedimentary Geology* 130, 65–80.

Kirkham, A., 2003. Glauconitic spherules from the Triassic of the Bristol area, SW England: probable microtektite pseudomorphs. *Proceedings of the Geologists' Association* 114, 11–21.

Kitamura, A., 1998. Glaucony and carbonate grains as indicators of the condensed section: Omma Formation, Japan. *Sedimentary Geology* 122, 151–163.

Knox, R.W.O.B., 1979. Igneous grains associated with zeolites in the Thanet Beds of Pegwell Bay, northeast Kent. *Proceedings of the Geologists' Association* 90, 55–59.

Kordi, M., Turner, B., Salem, A.M.K., 2011. Linking diagenesis to sequence stratigraphy in fluvial and shallow marine sandstones: evidence from the Cambrian–Ordovician lower sandstone unit in southwestern Sinai, Egypt. *Marine and Petroleum Geology* 28, 1554–1571.

Korkutis, V., 1981. Late Precambrian and Early Cambrian in the East European platform. *Precambrian Research* 15, 75–94.

Kossovskaya, A.G., Drits, V.A., 1970. The variability of micaceous minerals in sedimentary rocks. *Sedimentology* 15, 83–101.
Lantzsch, H., Hanebuth, T.J.J., Henrich, R., 2010. Sediment recycling and adjustment of deposition during deglacial drowning of a low-accumulation shelf (NW Iberia). *Continental Shelf Research* 30, 1665–1679.
Leckie, R.M., Bralower, T.J., Cashman, R., 2002. Oceanic anoxic events and plankton evolution: biotic response to tectonic forcing during the Mid-Cretaceous. *Paleoceanography* 17, 13–29.
Lee, C.H., Choi, S., Suh, M., 2002. High iron glaucony from the continental shelf of the Yellow Sea off the southwestern Korean Peninsula. *Journal of Asian Earth Science* 20, 507–515.
Lee, Y.I., Paik, I.S., 1997. High alumina glaucony from the Early Ordovician Mungok Formation, Korea. *Geoscience Journal* 1 (2), 108–114.
Legrand Sr., H.E., 1989. An innovative hydrogeologic setting for disposal of low-level radioactive wastes. *Environmental Geology and Water Sciences* 13 (3), 233–239.
Lewis, D.W., Belliss, S.E., 1984. Mid Tertiary unconformities in the Waitaki Subdivision, North Otago. *Journal of the Royal Society of New Zealand* 14 (3), 251–276.
Li, M.R., Wang, S.S., Qiu, J., 1996. The ages of glauconites from Tieling and Jingeryu Formations, Beijing–Tianjin Area. *Acta Petrologica Sinica* 12 (3), 416–423 (in Chinese with English abstract).
Li, X., Cai, Y., Hu, X., Huang, Z., Wang, J., 2012. Mineralogical characteristics and geological significance of Albian (Early Cretaceous) glauconite in Zanda, southwestern Tibet, China. *Clay Minerals* 47, 45–58.
Lim, D.I., Park, Y.A., Choi, J.Y., Chu, J.W., Khim, B.K., 2000. Glauconite grains in continental shelf sediments around the Korean Peninsula and their depositional implications. *Geo-Marine* 20, 80–86.
Lo, S.C., 1980. Microbial fossils from the lower Yudoma Suite, earliest Phanerozoic, eastern Siberia. *Precambrian Research* 13, 109–166.
Long, D.G.F., Yip, S.S., 2009. The Early Cambrian Bradore Formation of southeastern Labrador and adjacent parts of Quebec: architecture and genesis of clastic strata on an Early Paleozoic wave-swept shallow marine shelf. *Sedimentary Geology* 215, 50–69.
Longuépée, H., Cousineau, P.A., 2006. Constraints on the genesis of ferrian illite and aluminum-rich glauconite: potential impact on sedimentology and isotopic studies. *The Canadian Mineralogist* 44, 967–980.
Lorenzen, J., Kuhnt, W., Holbourn, A., Flögel, S., Moullade, M., Tronchetty, G., 2013. A new sediment core from the Bedoulian (Lower Aptian) stratotype at Roquefort-La Bédoule, SE France. *Cretaceous Research* 39, 6–16.
Loveland, P.J., 1981. Weathering of a soil glauconite in southern England. *Geoderma* 25, 35–54.
Lu, W., Smith, E.H., 1996. Modeling potentiometric titration behavior of glauconite. *Geochimica et Cosmochimica Acta* 60 (18), 3363–3373.
Lurcock, P.C., Wilson, G.S., 2013. The palaeomagnetism of glauconitic sediments. *Global and Planetary Change* 110, 278–288.
Ly, C.K., 1981. Sources of beach sand from the central and eastern coasts of Ghana, West Africa. *Marine Geology* 44, 229–240.
MacGregor, A.R., 1983. The Waitakere Limestone, a temperate algal carbonate in the lower Tertiary of New Zealand. *Journal of the Geological Society, London* 140, 387–399.
Mackenzie, K.J.D., Cardile, C.M., Brown, I.W.M., 1988. Thermal and mössbauer studies of iron-containing hydrous silicates: VII. Glauconite. *Thermochimica Acta* 136, 247–261.
Maher Jr., H.D., Hays, T., Shuster, R., Mutrux, J., 2004. Petrography of Lower Cretaceous sandstones on Spitsbergen. *Polar Research* 23 (2), 147–165.
Mancini, E.A., Tew, B.H., 1993. Eustasy versus subsidence: Lower Paleocene depositional sequences from southern Alabama, eastern Gulf Coastal Plain. *Geological Society of America Bulletin* 105, 3–17.
Marivaux, L., El Essid, M., Marzougui, W., Ammar, H.K., Adnet, S., Marandat, B., Merzeraud, G., Ramdarshan, A., Tabuce, R., Liaud, M.V., Yans, J., 2014. A morphological intermediate between Eosimiiform and Simiiform Primates from the Late Middle Eocene of Tunisia: Macroevolutionary and paleobiogeographic implications of Early Anthropoids. *American Journal of Physical Anthropology* 154, 387–401.
Martinec, P., Vavro, M., Scucka, J., Maslan, M., 2010. Properties and durability assessment of glauconitic sandstone: a case study on Zamel sandstone from the Bohemian Cretaceous Basin (Czech Republic). *Engineering Geology* 115, 175.
Martins, V., Abrantes, I., Granjeia, C., Martins, P., Nagai, R., Sousa, S.H.M., Laut, L.L.M., Dias, J.M.A., Dias, J.M., Silva, E.F., Rocha, F., 2012. Records of sedimentary dynamics in the continental shelf and upper slope between Aveiro–Espinho (N Portugal). *Journal of Marine Systems* 96–97, 48–60.
Mc Conchie, D.M., Lewis, D.W., 1980. Varieties of glauconite in Late Cretaceous and Early Tertiary rocks of the South Island of New Zealand and new proposals for classification. *New Zealand Journal of Geology and Geophysics* 23, 413–438.
McMaster, R.L., LaChance, T.P., 1968. Seismic reflectivity studies on northwestern African continental shelf, Strait of Gibraltar to Mauritania. *American Association of Petroleum Geologists Bulletin* 52, 2387–2396.
McRae, S.G., 1972. Glauconite. *Earth-Science Reviews* 8, 397–440.
McRae, S.G., Lambert, J.L.M., 1968. A study of some glauconites from Cretaceous and Tertiary formations in South-East England. *Clay Minerals* 7, 431–440.
Mei, M.X., Yang, F.J., Gao, J.H., Meng, Q.F., 2008. Glauconites formed in the high-energy shallow-marine environment of the Late Mesoproterozoic: a case study from Tieling Formation at Jixian section in Tianjin, North China. *Earth Science Frontiers* 15 (4), 146–158.
Mendes, I., Gonzalez, R., Dias, J.M.A., Lobo, F., Martins, V., 2004. Factors influencing recent benthic foraminifera distribution on the Guadiana shelf (southwestern Iberia). *Marine Micropaleontology* 51, 171–192.
Meng, X.Q., 2006. Geological characteristics and significance of glauconites in stromatolite rock-reef of Mesoproterozoic Tieling Formation in Jixian County. *Northwestern Geology* 3, 112–116 (in Chinese with English abstract).
Merriman, R.J., 1983. The origin of glauconitic material in Crag deposits from East Anglia. *Proceeding of Geologist's Association* 94 (1), 13–19.
Meshri, I.D., Comer, J.B., 1990. A subtle diagenetic trap in the Cretaceous glauconite sandstone of Southwest Alberta. *Earth Science Reviews* 29, 199–214.
Metwalli, M.H., Abdel-Hadi, Y.E., 1975. The significance of the variation of crude oil gravities of some oil fields in the Northern Western Desert, A. R. Egypt. In: *9th Arab Petroleum Congress, Dubai, 113(B-3), pp.1–10*.
Meunier, A., El Albani, A., 2007. The glauconite–Fe-illite–Fe-smectite problem: a critical review. *Terra Nova* 19, 95–104.
Michalík, J., Lintnerová, O., Reháková, D., Boorová, D., Simo, V., 2012. Early Cretaceous sedimentary evolution of a pelagic basin margin (the Manín Unit, central Western Carpathians, Slovakia). *Cretaceous Research* 38, 68–79.
Mishra, U.K., Sen, S., 2001. Dinosaur bones from Meghalaya. *Current Science* 80 (8), 1053–1056.
Misi, A., Azmy, K., Kaufman, A.J., Oliveira, T.F., Sanches, A.L., Oliveira, G.D., 2014. Review of the geological and geochronological framework of the Vazante sequence, Minas Gerais, Brazil: implications to metallogenic and phosphogenic models. *Ore Geology Reviews* 63, 76–90.

Misik, M., Sucha, V., 1994. Glauconite from the red nodular limestones of Jurassic age (Manin Gorge, western Carpathians). *Geologica Carpathica Clays* 1, 85–92.

Montag, R.L., Seidemann, D.E., 1981. A test of the reliability of Rb–Sr dates for selected glauconite morphologies of the Upper Cretaceous (Navesink Formation) of New Jersey. *Earth and Planetary Science Letters* 52, 285–290.

Morton, A.C., Merriman, R.J., Mitchell, J.G., 1984. Genesis and significance of glauconitic sediments of the Southwest Rockall Plateau. *Initial Reports of the Deep Sea Drilling Project* 81, 645–652.

Morton, J.P., Long, L.E., 1980. Rb–Sr dating of Paleozoic glauconite from the Llano region, Central Texas. *Geochimica et Cosmochimica Acta* 44, 663–672.

Muza, J.P., Wise Jr., S.W., 1983. An authigenic gypsum, pyrite, and glauconite association in a Miocene deep sea biogenic ooze from the Falkland Plateau, Southwest Atlantic Ocean. *Deep Sea Drilling Proceedings* 71, 361–375.

Najarro, M., Rosales, I., Chivelet, J.M., 2011. Major palaeoenvironmental perturbation in an Early Aptian carbonate platform: prelude of the Oceanic Anoxic Event 1a? *Sedimentary Geology* 235, 50–71.

Neill, G.M., Ruffell, A., 2004. Authigenic phosphate nodules (Late Cretaceous, northern Ireland) as condensed succession microarchives. *Cretaceous Research* 25, 439–452.

Nelson, C.S., Bornhold, B.D., 1984. Temperate continental shelf skeletal carbonate deposits. *Geobios* 17, 109–113.

Newman, T.G., Ghail, R.C., Skipper, J.A., 2013. Deoxygenated gas occurrences in the Lambeth Group of Central London, UK. *Quarterly Journal of Engineering Geology and Hydrogeology* 46, 167–177.

Nichols, G., 2012. *Sedimentology and Stratigraphy*, Second ed. Wiley-Blackwell. 419 p.

Obasi, C.C., Terry Jr., D.O., Myer, G.H., Grandstaff, D.E., 2011. Glauconite composition and morphology, shocked quartz, and the origin of the Cretaceous(?) Main Fossiliferous Layer (MFL) in southern New Jersey, USA. *Journal of Sedimentary Research* 81, 479–494.

Odin, G.S., Fullagar, P.D., 1988. Geological significance of the glaucony facies. In: Odin, G.S. (Ed.), *Green Marine Clays: Developments in Sedimentology*, vol. 45, pp. 295–332.

Odin, G.S., Létolle, R., 1980. *Glauconitization and Phosphatization Environments: a Tentative Comparison*, 29. SEPM Special Publications, pp. 227–237.

Odin, G.S., Matter, A., 1981. De Glauconiarum Origine. *Sedimentology* 28, 611–641.

Odin, G.S., Velde, B., Bonhomme, M., 1977. Radiogenic argon in glauconites as a function of mineral recrystallization. *Earth and Planetary Science Letters* 37 (1), 154–158.

Odom, I.E., 1976. Microstructure, mineralogy and chemistry of Cambrian glauconite pellets and glauconite, Central USA. *Clays and Clay Minerals* 24, 232–238.

Odom, I.E., 1984. Glauconite and celadonite minerals. In: Bailey, S.W. (Ed.), *Reviews in Mineralogy*, 13. MICAS, pp. 545–572.

Olsson, R.K., 1989. Depositional sequences in the Cretaceous post-rift sediments on the New Jersey Atlantic margin. Studies related to continental margins. *Marine Geology* 90, 113–118.

Orberger, B., Pagel, M., 2000. Diagenetic evolution of Cretaceous siltstones from drill core MAR 501 (South-Eastern France). *Journal of Geochemical Exploration* 69–70, 115–118.

Ostwald, J., 1990. The biogeochemical origin of the Groote Eylandt manganese oxide pisoliths and ooliths, northern Australia. *Ore Geology Review* 5, 469–490.

Özgüner, A.M., Varol, B., 2009. The genesis, mineralization, and stratigraphic significance of phosphatic/glauconitic condensed limestone unit in the Manavgat Basin, SW Turkey. *Sedimentary Geology* 221, 40–56.

Parize, O., Fiet, N., Friès, G., Imbert, P., Latil, J.L., Rubino, J.L., Viana, A., 2005. Depositional dynamics of glaucony-rich deposits in the Lower Cretaceous of the Nice arc, southeast France. *Cretaceous Research* 25, 179–189.

Parker, R.J., 1975. The petrology and origin of some glauconitic and glauco-conglomeratic phosphorites from the South African continental margin. *Journal of Sedimentary Petrology* 45, 230–242.

Parrish, J.T., Droser, M.L., Bottjer, D.J., 2001. A Triassic upwelling zone: the Shublik Formation, Arctic Alaska, USA. *Journal of Sedimentary Research* 71, 272–285.

Parron, C., Amouric, M., 1990. Crystallochemical heterogeneity of glauconites and the related problem of glauconite-celadonite distinction. *Chemical Geology* 84, 286–289.

Parry, W.T., Reeves, C.C., 1966. Lacustrine Glauconitic mica from pluvial lake Mound, Lynn and Terry counties, Texas. *The American Mineralogist* 51, 229–235.

Pasquini, C., Lualdi, A., Vercesi, P., 2004. Depositional dynamics of glaucony-rich deposits in the Lower Cretaceous of the Nice Arc, Southeast France. *Cretaceous Research* 25, 179–189.

Peters, S.E., Gaines, R.R., 2012. Formation of the 'Great Unconformity' as a trigger for the Cambrian explosion. *Nature* 484, 363–366.

Plint, A.G., 1983. Facies, environments and sedimentary cycles in the Middle Eocene, Bracklesham Formation of the Hampshire Basin: evidence for global sea-level changes? *Sedimentology* 30, 625–653.

Porrenga, D.H., 1967. Glauconite and chamosite as depth indicators in the marine environment. *Marine Geology* 5, 495–501.

Porrenga, D.H., 1968. Non-marine glauconitic illite in the Lower Oligocene of Aardebrug, Belgium. *Clay Minerals* 7, 421–430.

Prélat, A., Hodgson, D.M., Hall, M., Jackson, C.A.L., Baunack, C., Tveiten, B., 2015. Constraining sub-seismic deep-water stratal elements with electrofacies analysis: a case study from the Upper Cretaceous of the Måløy Slope, offshore Norway. *Marine and Petroleum Geology* 59, 268–285.

Purdy, C.B., Mignerey, A.C., Helz, G.R., Drummond, D.D., Kubik, P.W., Elmore, D., Hemmick, T., 1987. 36 Cl: a tracer in groundwater in the Aquia Formation of Southern Maryland. *Nuclear Instruments and Methods in Physics Research Section B: Beam Interactions with Materials and Atoms* 29, 372–375.

Rao, V.P., Lamboy, M., Dupeuble, P.A., 1993. Verdine and other associated authigenic (glaucony, phosphate) facies from the surficial sediments of the southwestern continental margin of India. *Marine Geology* 111, 133–158.

Rao, V.P., Thamban, M., Lamboy, M., 1995. Verdine and glaucony facies from surficial sediments of the eastern continental margin of India. *Marine Geology* 127, 105–113.

Rasmussen, E.S., Dybkjaer, K., 2005. Sequence stratigraphy of the Upper Oligocene–Lower Miocene of eastern Jylland, Denmark: role of structural relief and variable sediment supply in controlling sequence development. *Sedimentology* 52, 25–63.

Rasser, M.W., Piller, E.W., 2004. Crustose algal frameworks from the Eocene Alpine Foreland. *Palaeogeography, Palaeoclimatology, Palaeoecology* 206, 21–39.

Rathore, S.S., Prabhu, B.N., Vijan, A.R., Vic, K.C., Misra, K.N., 1999. K–Ar age of Ukra glauconites from the Kutch Basin, India. *Proceedings of the Indian Academy of Sciences-Earth and Planetary Sciences* 108, 49–55.

Rawlley, R.K., 1994. Mineralogical investigations on an Indian glauconitic sandstone of Madhya Pradesh State. *Applied Clay Science* 8, 449–465.

Rea, D.K., Dehn, J., Driscoll, N.W., Farrell, J.W., Janecek, T.R., Pospichal, R.J.J., Resiwati, P., 1990. Paleoceanography of the

eastern Indian Ocean from ODP Leg 121 drilling on Broken Ridge. *Bulletin of Geological Society of America* 102, 679–690.
Reeder, S.W., Hitchon, B., Levinson, A.A., 1972. Hydrogeochemistry of the surface waters of the Mackenzie River drainage basin, Canada — I. Factors controlling inorganic composition. *Geochimica et Cosmochimica Acta* 36, 325–865.
Reid, C.M., James, N.P., Beauchamp, B., Kyser, T.K., 2007. Faunal turnover and changing oceanography: Late Palaeozoic warm-to-cool water carbonates, Sverdrup Basin, Canadian Arctic Archipelago. *Palaeogeography, Palaeoclimatology, Palaeoecology* 249, 128–159.
Retzler, A., Wilson, M.A., Avni, Y., 2013. Chondrichthyans from the Menuha Formation (Late Cretaceous: Santonian–Early Campanian) of the Makhtesh Ramon region, southern Israel. *Cretaceous Research* 40, 81–89.
Reynolds, R.C., 1963. Potassium-rubidium ratios and polymorphism in illites and microclines from the clay size fractions of proteroeoic carbonate rocks. *Geochimica et Cosmochimica Acta* 27, 1097–1112.
Richards, J.R., Gee, R.D., 1985. Galena lead isotopes from the eastern part of the Nabberu Basin, Western Australia. *Australian Journal of Earth Sciences* 32 (1), 47–54.
Riedinger, N., Pfeifer, K., Kasten, S., Garming, J.F.L., Vogt, C., Hensen, C., 2005. Diagenetic alteration of magnetic signals by anaerobic oxidation of methane related to a change in sedimentation rate. *Geochimica et Cosmochimica Acta* 69 (16), 4117–4126.
Rifai, I.R., Shaaban, M.N., 2007. Authigenic dolomite cementation in the Upper Cretaceous Phosphate Formation, Western Desert, Egypt. *Sedimentary Geology* 202, 702–709.
Roban, R., Dobrinescu, M.C.M., 2012. Lower Cretaceous lithofacies of the black shales rich Audia Formation, Tarcau Nappe, eastern Carpathians: genetic significance and sedimentary palaeoenvironments. *Cretaceous Research* 38, 52–67.
Robert, M., 1973. The experimental transformation of mica toward smectite; relative importance of total charge and tetrahedral substitution. *Clays and Clay Minerals* 21, 167–174.
Rolf, R.M., Kimball, C.W., Odom, I.E., 1977. Mossbauer characteristics of Cambrian glauconite, central USA. *Clays and Clay Minerals* 25, 131–137.
Rongchuan, L., Shixin, W., Yuanfu, H., Weimin, D., Lirong, C., 1986. A Mössbauer investigation of the formation process of glauconite. *Hyperfine Interactions* 29 (1–4), 1085–1088.
Rothe, P., 1973. Sedimentation in the deep-sea areas adjacent to the Canary and Cape Verde islands. *Marine Geology* 14, 191–206.
Rousset, D., Leclerc, S., Clauer, N., Lancelot, J., Cathelineau, M., Aranyossy, J.F., 2004. Age and origin of Albian glauconites and associated clay minerals inferred from a detailed geochemical analysis. *Journal of Sedimentary Research* 74 (5), 631–642.
Saha, O., Shukla, U.K., Rani, R., 2010. Trace fossils from the Late Cretaceous Lameta Formation, Jabalpur Area, Madhya Pradesh: paleoenvironmental implications. *Journal Geological Society of India* 76, 607–620.
Saito, Y., Nishimura, A., Matsumoto, E., 1989. Transgressive sand sheet covering the shelf and upper slope off Sendai, Northeast Japan. *Marine Geology* 89, 245–258.
Salamon, M.A., 2007. First record of bourgueticrinid crinoids from the Cenomanian of southern Poland. *Cretaceous Research* 28, 495–499.
Samanta, A., Sarkar, A., Bera, M.K., Rai, J., Rathore, S.S., 2013. Late Paleocene–Early Eocene carbon isotope stratigraphy from a near-terrestrial tropical section and antiquity of Indian mammals. *Journal of Earth System Science* 122, 163–171.
Sánchez-Navas, A., Algarra, A.M., Eder, V., Reddy, B.J., Nieto, F., Zanin, Y.N., 2008. Color, mineralogy and composition of Upper Jurassic West Siberian glauconite: useful indicators of paleoenvironment. *The Canadian Mineralogist* 46, 1545–1564.
Sánchez-Navas, A., Algarra, M.A., Nieto, F., 1998. Bacterially-mediated authigenesis of clays in phosphate stromatolites. *Sedimentology* 45, 519–533.
Saraev, S.V., Baturina, T.P., 2008. Lithology and geochemistry of Triassic deposits in the southwest of the West Siberian geosyneclise. *Russian Geology and Geophysics (Geologiya i Geofizika)* 49 (6), 357–370 (477–494).
Sarkar, S., Choudhuri, A., Banerjee, S., Van Loon (Tom), A.J., Bose, P.K., 2014. Seismic and non-seismic soft-sediment deformation structures in the Proterozoic Bhander Limestone, central India. *Geologos* 20 (2), 89–103.
Sarma, J.N., Basumallick, S., 1979. Glauconite in some Eocene carbonate rocks of Mikir hills, Assam. *Indian Journal of Earth Sciences* 6, 186–190.
Sarmah, R.K., Borgohain, R., 2012. Lithostratigraphy of the Paleogene shelf sediments in Assam and Meghalaya — a review. *Indian Streams Research Journal* 12, 1–4.
Schulz, H.D., Zabel, M., 2006. Marine Geochemistry. Springer, Berlin.
Schweitzer, C.E., Ćosović, V., Feldmann, R.M., 2005. Harpactocarcinus from the Eocene of Istria, Croatia, and the paleoecology of the Zanthopsidae (Crustacea: Decapoda: Brachyura). *Journal of Paleontology* 79 (4), 663–669.
Seed, D.P., 1965. The formation of vermicular pellets in New Zealand glauconites. *The American Mineralogist* 50, 1097–1106.
Selby, D., 2009. U–Pb zircon geochronology of the Aptian/Albian boundary implies that the GL-O international glauconite standard is anomalously young. *Cretaceous Research* 30, 1263–1267.
Sepkoski, J.J., 2000. Crustacean biodiversity through the marine fossil record. *Contributions to Zoology* 69, 213–221.
Sharafi, M., Mahboubi, A., Moussavi-Harami, R., Ashuri, M., Rahimi, B., 2013. Sequence stratigraphic significance of sedimentary cycles and shell concentrations in the Aitamir Formation (Albian–Cenomanian), Kopet-Dagh Basin, northeastern Iran. *Journal of Asian Earth Sciences* 67–68, 171–186.
Singh, I.B., Kumar, S., 1978. On the stratigraphy and sedimentation of the Vindhyan sediments in the Chitrakut area, Banda District (U.P.)–Sama District (M.P. *Journal of Geology Society of India* 19, 359–367.
Skiba, M., Szeliga, K.M., Szymański, W., Błachowski, A., 2014. Weathering of glauconite in soils of temperate climate as exemplified by a Luvisol profile from Góra Puławska, Poland. *Geoderma* 235–236, 212–226.
Sluijs, A., van Roij, L., Harrington, G.J., Schouten, S., Sessa, J.A., LeVay, L.J., Reichart, G.J., Slomp, C.P., 2014. Extreme warming, photic zone euxinia and sea level rise during the Paleocene/Eocene thermal maximum on the Gulf of Mexico Coastal Plain; connecting marginal marine biotic signals, nutrient cycling and ocean deoxygenation. *Climate of the Past* 10, 1421–1439.
Smalley, P.C., Forsberg, A., Rundberg, Y., Raheim, A., 1986. Rb–Sr glauconite systematics during diagenesis and the dating of fluid movement. *Terra Cognita* 6, 207.
Smith, E.H., Lu, W., Vengris, T., Binkiene, R., 1996. Sorption of heavy metals by Lithuanian glauconite. *Water Research* 30 (12), 2883–2892.
Sorrentino, L., Stilwell, J., Mays, C., 2014. A model of tephra dispersal from an Early Palaeogene shallow submarine Surtseyan-style eruption(s), the Red Bluff Tuff Formation, ChathamIsland, New Zealand. *Sedimentary Geology* 300, 86–102.
Sprong, J., Kouwenhoven, T.J., Bornemann, A., Dupuis, C., Speijer, R.P., Stassen, P., Steurbaut, E., 2013. In search of the Latest Danian Event in a paleobathymetric transect off

Kasserine Island, north-central Tunisia. *Palaeogeography, Palaeoclimatology, Palaeoecology* 379–380, 1–16.
Srasra, E., Trabelsi-Ayedi, M., 2000. Textural properties of acid activated glauconite. *Applied Clay Science* 17, 71–84.
Stassen, P., Dupuis, C., Steurbaut, E., Yans, J., Speijer, R.P., 2012. Perturbation of a coastal Tethyan environment during the Paleocene–Eocene thermal maximum in Tunisia (Sidi Nasseur and Wadi Mezaz). *Palaeogeography, Palaeoclimatology, Palaeoecology* 317–318, 66–92.
Stassen, P., Thomas, E., Speijer, R.P., 2015. Paleocene–Eocene thermal maximum environmental change in the New Jersey Coastal Plain: Benthic foraminiferal biotic events. *Marine Micropaleontology* 115, 1–23.
Stille, P., Fischer, H., 1990. Secular variation in the isotopic composition of Nd in Tethys seawater. *Geochimica et Cosmochimica Acta* 54, 3139–3145.
Strasser, A., Aurell, M., Bádenas, B., Meléndez, G., Tomás, S., 2005. From platform to basin to swell: orbital control on sedimentary sequences in the Oxfordian, Spain. *Terra Nova* 17 (5), 407–413.
Strickler, M.E., Ferrell Jr., R.E., 1990. Fe substitution for Al in glauconites with increasing diagenesis in the first Wilcox sandstone (Lower Eocene), Livingstone Parish, Louisiana. *Clays and Clay Minerals* 38, 69–76.
Tazaki, K., Fyfe, W.S., 1992. Microbial green marine clay from Izu-Bonin (west Pacific) deep-sea sediments. *Chemical Geology* 102, 105–118.
Tewari, V.C., Lokho, K., Kumar, K., Siddaiah, N.S., 2010. Late Cretaceous–Paleogene basin architecture and evolution of the Shillong shelf sedimentation, Meghalaya, northeast India. *Journal of Indian Geological Congress* 2, 61–73.
Thompson, G.R., Hower, J., 1975. The mineralogy of glauconite. *Clays and Clay Minerals* 23, 289–300.
Tlig, S., Sahli, S., Er-Raioui, L., Alouani, R., Mzoughi, M., 2010. Depositional environment controls on petroleum potential of the Eocene in the North of Tunisia. *Journal of Petroleum Science and Engineering* 71, 91–105.
Tóth, E., Weiszburg, T.G., Jeffries, T., Williams, C.T., Bartha, A., Bertalan, E., Cora, I., 2010. Submicroscopic accessory minerals overprinting clay mineral REE patterns (celadonite–glauconite group examples). *Chemical Geology* 269, 312–328.
Vail, P.R., Mitchum Jr., R.M., Todd, R.G., Widmier, J.M., Thompson, S.I., Sangree, J.B., Bubb, J.N., Hatlelid, W.G., 1977. Seismic stratigraphy and global changes of sea level. In: Payton, C.E. (Ed.), *Seismic Stratigraphy–Applications to Hydrocarbon Exploration, American Association of Petroleum Geologists Memoir*, 26, pp. 49–212.
Valanciene, V., Siauciunas, R., Valancius, Z., 2014. Evaluation of glauconite rock color stability during firing. *Applied Clay Science* 99, 110–118.
Van Delft, F.C.M.J.M., Den Hartog, A.J., Ijdo, D.J.W., Ponec, V., Vurens, G.H., Van Der Kraan, A.M., 1990. Oxidation and dehydrogenation of alcohols by glauconite, a natural Fe(II)- and Fe(III)-containing sheet silicate, and Ferri-sepiolite, its molecular sieve analogue. *Journal of Molecular Catalysis* 60, 109–125.
Van Houten, F.B., Purucker, M.E., 1984. Glauconitic peloids and chamositic ooids–favorable factors, constraints, and problems. *Earth-Science Reviews* 20, 211–243.
Vandenberghe, N., Burleigh, H.W., Wampler, J.M., Houthuys, R., Louwye, S., Adriaens, R., Vos, K., Lanckacker, T., Matthijs, J., Deckers, J., Verhaegen, J., Laga, P., Westerhoff, W., Munsterman, D., 2014. The implications of K–Ar glauconite dating of the Diest formation on the paleogeography of the Upper Miocene in Belgium. *Geologica Belgica* 17, 161–174.
Vander Lingeb, G.J., Smale, D., Lewis, D.W., 1978. Alteration of a pelagic chalk below a paleokarst surface, Oxford, South Island, New Zealand. *Sedimentary Geology* 21, 45–66.
Varol, B., Özgüner, A.M., Koşun, E., İmamğolu, Ş., Daniş, M., Karakullukçu, T., 2000. Depositional environments and sequence stratigraphy of glauconites of western Black Sea region. *Mineral Research and Exploration Bulletin* 122, 1–21.
Vasković, N., Jović, V., Matović, V., 2010. Early Cretaceous glauconite formation and Late Cretaceous magmatism and metallogeny of the East Serbian part of the Carpatho–Balkanides. *Acta Mineralogica-Petrographica, Field Guide Series* 25, 1–32.
Vaz, G.G., 2000. Verdine and glaucony facies from continental margin off Chennai, Bay of Bengal. *Journal of the Geological Society of India* 55, 297–306.
Vecsei, A., 1998. A sandy tidal coast in the uppermost Muschelkalk and the origin of the Muschelkalk/Keuper boundary in the southwestern Germanic basin. *Geologische Rundschau* 86, 835–851.
Velde, B., 1985. Clay minerals: a physicochemical explanation of their occurrence. *Developments in Sedimentology* 40, 427.
Velde, B., Medhioub, M., 1988. Approach to chemical equilibrium in diagenetic chlorites. *Contributions to Mineralogy and Petrology* 98, 122–127.
Viira, V., Mens, K., Nemliher, J., 2006. Lower Ordovician Leetse Formation in the North Estonian Klint area. *Proceedings of the Estonian Academy of Sciences, Geology* 55 (2), 156–174.
Vijan, A.R., Rathore, S.S., Vig, K.C., Bansal, M., Singh, M.P., Prabhu, B.N., 2000. K–Ar and Rb–Sr ages of Cretaceous glauconites from Jaisalmer Basin, Rajasthan. *Journal of the Geological Society of India* 56, 15–25.
Walker, R.G., Bergman, K.M., 1993. Shannon Sandstone in Wyoming: a shelf-ridge complex reinterpreted as lowstand shoreface deposits. *Journal of Sedimentary Research* 63, 839–851.
Wang, J.T., Zhang, Y.S., Song, T.R., 2011. Characteristics and sedimentary environment of authigenic glauconite from limestone of the Amushan Formation in Xi Ujimqin Banner, Inner Mongolia. *Acta Petrologica Et Mineralogica* 2, 259–266 (in Chinese with English abstract).
Wang, Q., Zhu, E.Q., Zhang, J.H., Feng, W.W., 1985. The assemblage of authigenic iron minerals in superficial sediments of the Sanya Bay, Hainan Island. *Acta Geologica Sinica* 59 (4), 293–303 (in Chinese with English abstract).
Wang, Y.H., 1983. Discovery and primary study of glauconite in modern lacustrine sediments from Fuxian Lake. *Chinese Science Bulletin* 28, 1388–1392.
Webb, A.W., Mcdougall, I., Cooper, J.A., 1963. Retention of radiogenic argon in glauconites from Proterozoic sediments, northern Territory Australia. *Nature* 199, 270–271.
Wermunde, G., 1961. Glauconite in Early Tertiary sediments of Gulf Coastal Province. *American Association of Petroleum Geologists Bulletin* 45, 1667–1696.
Whiteside, D.I., Robinson, D., 1983. A glauconitic clay-mineral from a speleological deposit of Late Triassic age. *Palaeogeography, Palaeoclimatology, Palaeoecology* 41, 81–85.
Wigley, R., Compton, J.S., 2007. Oligocene to Holocene glauconite–phosphorite grains from the Head of the Cape Canyon on the western margin of South Africa. *Deep-Sea Research II* 54, 1375–1395.
Wilmsen, M., Niebuhr, B., Hiss, M., 2005. The Cenomanian of northern Germany: facies analysis of a transgressive biosedimentary system. *Facies* 51, 242–263.
Witts, J.D., Bowman, V.C., Wignall, P.B., Crame, J.A., Francis, J.E., Newton, R.J., 2015. Evolution and extinction of Maastrichtian (Late Cretaceous) cephalopods from the López de Bertodano Formation, Seymour Island, Antarctica. *Palaeogeography, Palaeoclimatology, Palaeoecology* 418, 193–212.

Wood, J.M., Hopkins, J.C., 1992. Traps associated with paleovalleys and interfluves in an unconformity bounded sequence: lower Cretaceous Glauconitic Member, Southern Alberta, Canada. *Bulletin of American Association of Petroleum Geologists* 76, 904–926.

Wortmann, U.G., Herrle, J.O., Weissert, H., 2004. Altered carbon cycling and coupled changes in Early Cretaceous weathering patterns: evidence from integrated carbon isotope and sandstone records of the western Tethys. *Earth and Planetary Science Letters* 220, 69–82.

Wu, F.D., Lu, Y.C., Chen, P., Zhou, P., 1997. The discovery and significance of glauconites in the Huagong Formation of the Oligocene, Xihu Depression, East China Sea. *Acta Sedimentologica Sinica* 15 (3), 158–161 (in Chinese with English abstract).

Xie, G.C., 1991. A discovery and primary study of glauconite in the Upper Triassic Yanchang oil-bearing sandstone in northern Shaanxi. *Chinese Journal of Geology* 26, 129–136 (in Chinese with English abstract).

Xu, Y.H., 2010. The discovery and geological significance of glauconites from the Palaeoproterozoic Xiong'er Group in the southern part of the North China Craton. *Acta Sedimentologica Sinica* 28 (4), 671–675 (in Chinese with English abstract).

Yilmaz, I.O., Altiner, D., Tekin, U.K., Ocakoglu, F., 2012. The first record of the "mid-Barremian" Oceanic Anoxic Event and the late Hauterivian platform drowning of the Bilecik platform, Sakarya Zone, western Turkey. *Cretaceous Research* 38, 16–39.

Zachos, J.C., Schouten, S., Bohaty, S., Quattlebaum, T., Sluijs, A., Brinkhuis, H., Gibbs, S.J., Bralower, T.J., 2006. Extreme warming of mid-latitude coastal ocean during the Paleocene–Eocene thermal maximum: inferences from TEX86 and isotope data. *Geology* 34, 737–740.

Zaitseva, T.S., Ivanovskaya, T.A., Gorokhov, I.M., Yakovleva, O.V., Ku-tyavin, E.P., Mel'nikov, N.N., Kuznetsov, A.B., 2000. The Rb–Sr age and NGR spectra of glauconites from the Upper Riphean UK Formation, Southern Urals. In: *Isotope Dating of Geologic Processes: New Methods and Results*. GEOS, Moscow, pp. 144–147 (in Russian).

Zalat, A.A., Zaid, S.M., Gadallah, M.H., Abdel-Aziz, Z.A., 2012. Sandstones reservoir quality of the Matulla Formation, Gulf of Suez, Egypt. *Australian Journal of Basic and Applied Sciences* 6 (12), 511–529.

Zhou, X.Q., Li, N., Liang, G.S., Li, L., Tang, D.J., Fu, X.M., 2009. Sedimentary significance of the autochthonous glauconite in stromatolitic limestones of the Mesoproterozoic Tieling Formation in Jixian, Tianjin, North China. *Geological Bulletin of China* 7, 985–990 (in Chinese with English abstract).